The first original version of this manuscript has been submitted on May 31, 2025, for consideration in the peer-reviewed *Energy Conversion and Management* journal. Please note that the manuscript has not undergone peer review yet and has not been formally accepted for publication. Subsequent versions of this manuscript may have slightly different content. Please feel free to contact any of the authors; we welcome feedback.

Optimisation of Agrivoltaic Systems within the Water-Energy-Food Nexus

Sebastian Zainali[1,*], Silvia Ma Lu[1], Yuri Bellone[2], Pietro Elia Campana[1,*]

1 Mälardalen University, Department of Sustainable Energy Systems, Västerås SE 72123, Sweden

2 Università Cattolica del Sacro Cuore, Department of Sustainable Crop Production, Piacenza, Italy

Corresponding authors: sebastian.zainali@mdu.se, pietro.campana@mdu.se

Abstract

Agrivoltaic (APV) systems, which co-locate photovoltaic (PV) panels with agricultural production, have emerged as a promising strategy to simultaneously address water, energy, and food sustainability challenges. However, the optimal design of such systems remains complex due to competing objectives, site-specific conditions, and increasingly stringent policy constraints. This study presents a multi-objective optimisation framework for APV systems design that integrates climatic variability, crop performance modelling, PV system behaviour, and national policy thresholds with a water-energy-food (WEF) nexus approach. Using a genetic algorithm (GA) as the optimisation technique, the model explores optimal configurations of three APV system types: vertical, one-axis tracking, and overhead fixed-tilt. The optimisation considers four design parameters including module tilt, azimuth orientation, row pitch, and system height. Simulations are carried out at three geographically diverse European locations: Sweden, Germany, and Italy, over a six-year crop rotation period. The framework incorporates constraints from Swedish subsidy requirements, German yield retention standards, and Italian guidelines. A composite WEF index enables flexible prioritisation among objectives and reveals strong trade-offs between energy conversion and crop productivity (correlation ≈ -0.99). The results demonstrate that combining national policies with recommended best practices can render APV deployment practically infeasible at the development stage if no accurate APV integrated models are available to clearly depict the impact of shading on microclimate and crop growth. The row pitch emerged as the most influential design variable, with optimal spacing between 5–10 meters depending on location and constraints. Furthermore, the land equivalent ratio (LER) for crops can vary by up to 10% depending solely on interannual weather variability.

Keywords: Agrivoltaics; Water-Energy-Food Nexus; Multi-objective Optimisation; Policy Constraints; Crop Modelling; Land-Use Efficiency

1 Introduction

The water-energy-food (WEF) nexus has emerged as a critical framework for addressing global sustainability challenges, emphasising the interdependence of resource systems and the need for integrated management strategies [1–3]. In this context, agrivoltaic (APV) systems, the co-location of photovoltaic (PV) panels with agriculture, have gained attention as a promising solution aligning the WEF objectives [4]. By enabling simultaneous crop cultivation and solar energy conversion on the same land, APV systems offer a dual-use approach that optimises land resources and addresses multiple sustainability goals [5–7]. Notably, the integration of PV panels into farmland can yield synergetic benefits: the partial shade from panels reduces soil evaporation and influences local microclimate dynamics, leading to improved soil moisture retention and crop protection against extreme heat or weather [8,9]. These advantages make APV especially valuable in water-scarce regions and other challenging climates, where conserving water and maintaining food production are paramount [10]. Furthermore, by producing renewable electricity alongside crops, APV systems enhance overall land-use efficiency and bolster all three pillars of the WEF nexus, helping to secure food, generate clean electricity, and save water on the same piece of land [11]. Studies have reported that such dual-use systems can boost combined land productivity by dozens of percent compared to separate farming and solar installations. For instance, overall output gains on the order of 35–73% have been observed under favourable conditions [12]. In some cases, the microclimate benefits are so pronounced that certain crops yield significantly more under PV arrays. A field trial in an arid climate showed chilli and tomato production increasing threefold and twofold, respectively, under solar panels (with substantially less water use), thanks to reduced heat stress and improved water retention [4].

Real-world applications of APV underscore its potential within the WEF nexus across diverse settings. In arid regions like Jordan, APV projects have demonstrated enhanced water-use efficiency and sustained crop yields, while simultaneously contributing to renewable energy targets [10]. Specifically, the study estimated that covering approximately 50% of the currently irrigated summer tomato fields with PV panels could meet Jordan's target of generating 50% of its electricity from renewable energy sources, while also reducing national water consumption by an estimated 4–8.6%, highlighting APV's strategic value for water-limited agriculture [10]. In densely populated urban areas, innovative APV implementations are being explored on rooftops to address land scarcity. For example, a pilot in Shenzhen, China, demonstrated that rooftop APV could meet the city's entire demand for lettuce while also generating substantial electricity, providing a dual benefit for urban sustainability [13]. Likewise, in Europe, experimental APV farms have reported land-equivalent ratios well above 1 (meaning the combined output of food and energy exceeds that of separate uses of land), even reaching values approaching 1.6–1.8 in some cases [14]. These cases illustrate how APV can be adapted to different contexts, from water-constrained rural farms to space-constrained cities, to jointly advance food security and clean energy conversion. They also reinforce that the magnitude of APV benefits is site-specific, influenced by local climate, crop selection and management practices.

Despite these clear advantages, APV systems face important limitations and design challenges that must be addressed to fully realise their promise. A primary concern is the trade-off between solar panel shading and crop productivity: while shade can benefit certain crops and save water, it inherently reduces the sunlight available for photosynthesis, which may decrease yields for light-demanding crops [5]. The extent of this yield reduction depends on crop varieties, panel configuration (e.g., height, row spacing, orientation), and local environmental conditions [15,16]. Careful crop selection is therefore crucial, shade-tolerant or understory crops (such as leafy greens) may thrive beneath panels, whereas sun-loving staples might suffer without sufficient light [12]. APV systems are typical examples of a multi-objective optimisation problem, where both energy- and crop targets depend on the PV geometrical parameters [17]. For instance, denser or optimally tilted PV arrays can maximise energy output but will cast more shade on the ground, whereas more widely spaced or vertically oriented panels provide more uniform light for crops at the cost of lower total PV conversion [18]. A recent study has highlighted these design trade-offs. An east–west oriented PV arrangement was found to distribute light most evenly for crops, improving under-panel growth, but this configuration yielded less electricity overall compared to a conventional south-facing layout [18]. Such findings underscore that there is no one-size-fits-all APV design, the optimal configuration depends on site-specific factors like latitude, climate, and crop type. Moreover, performance can vary significantly from year to year: in Germany, the relative land productivity gains from APV were modest in normal weather years (~1.6× higher than separate land use) but spiked to nearly 1.9× during an unusually hot, dry year when the shade benefit to crops was greatest [19]. This variability highlights the importance of accounting for different climatic conditions and temporal patterns when evaluating APV systems. In summary, the key limitation is that without thoughtful design and management, APV could lead to suboptimal outcomes, either underperforming on energy yield or undermining crop production, if the shading, spacing and other parameters are not well balanced for the given environment. This recognition has driven a need for optimisation strategies that can navigate the complex trade-offs inherent in APV design.

To address these challenges, this study develops a comprehensive optimisation framework for APV system design, with a focus on maximising the co-benefits within the WEF nexus while mitigating the aforementioned trade-offs. In contrast to previous APV studies that often examine a single crop, location or year [20,21], our approach evaluates multiple cropping systems over several years and across diverse European climates, thereby capturing a broader range of conditions and interannual variability. This expanded scope, which includes a multi-year, multi-crop, and multi-location analysis, represents a novel contribution, as few studies to date have simultaneously assessed APV performance across such varied contexts. A multi-objective genetic algorithm (GA) is employed to explore the design space and identify optimal system configurations that jointly satisfy food and energy conversion goals (and implicitly water conservation goals), reflecting the integrated priorities of the WEF nexus. Notably, the optimisation incorporates regulatory constraints into the design criteria, an aspect often overlooked in prior research. In our framework, such policy constraints, including limits on land occupation and minimum required PV output, are embedded as boundary conditions to ensure that the resulting APV designs are not only theoretically optimal but also compliant with current APV regulations. By integrating these technical, agronomic, and policy considerations, the study advances the state of APV research toward more practically applicable solutions.

2 Methodology

The workflow consists of three main steps (1) data acquisition and preprocessing, (2) sensitivity analysis and optimisation using GA, (3) metric evaluation based on key performance indicators (KPIs), including land equivalent ratio (LER) (i.e., combination of energy conversion and crop yield), and water consumption. A schematic representation of the workflow is provided in Figure 1.

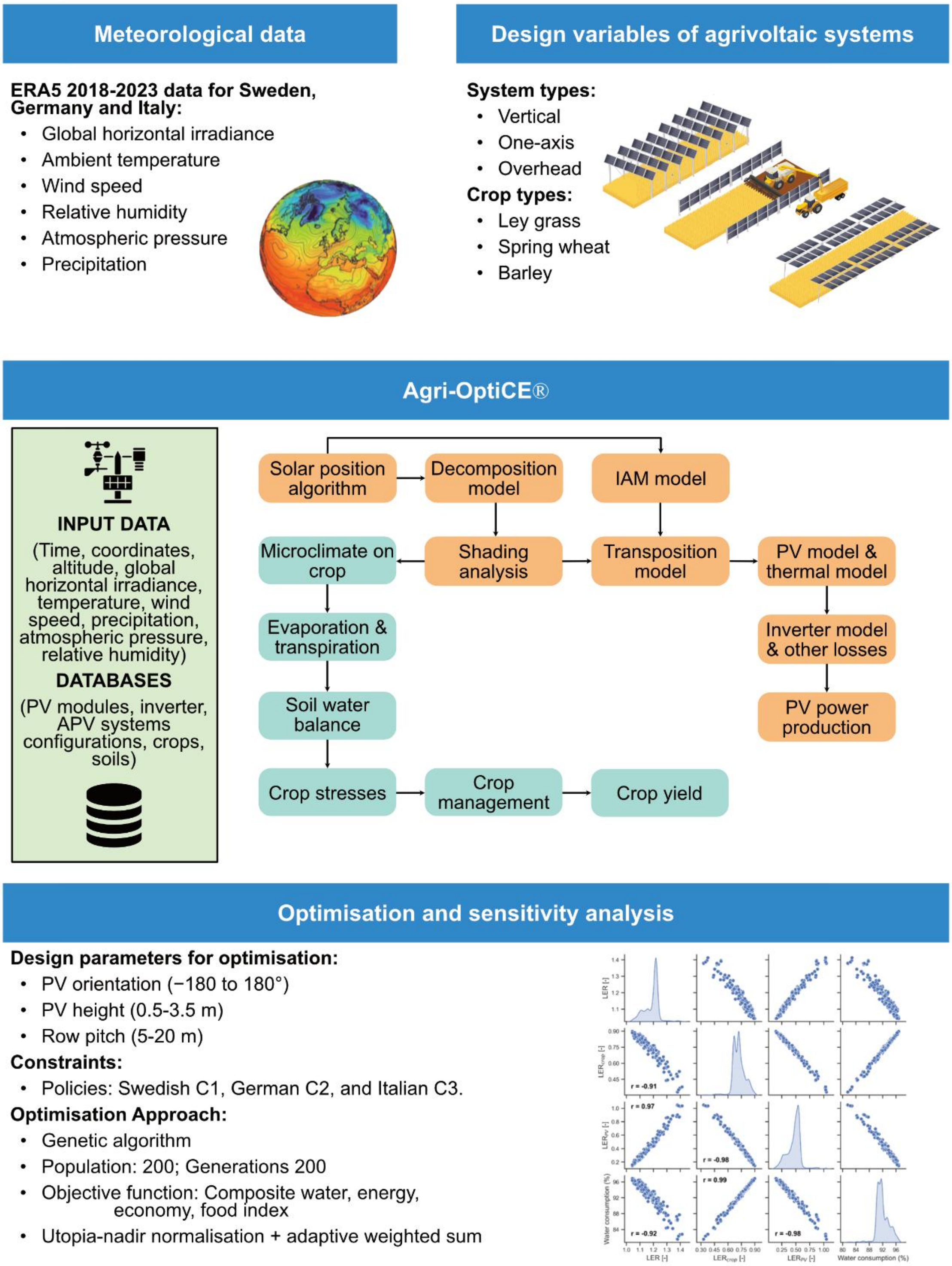

Figure 1. Overview of the optimisation framework and methodology used in the study.

2.1 Data acquisition and processing

The study considers three locations across different European climates: Kärrbo Prästgård, Sweden (59.5549°N, 16.7585°E), Jeggeleben, Germany (52.7305°N, 11.0285°E), and Piacenza, Italy (45.0524°N, 9.6923°E) (Figure 2).

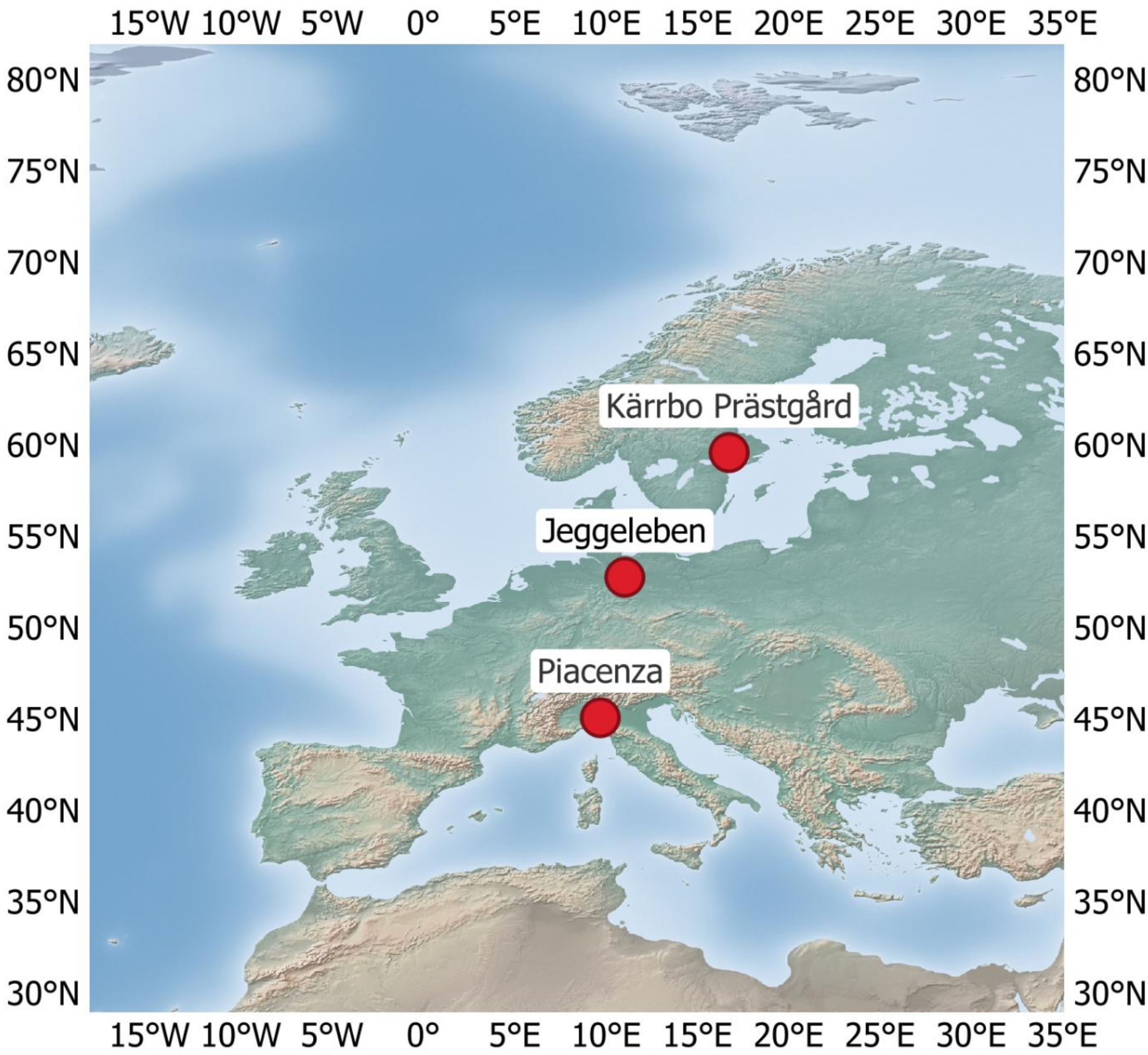

Figure 2. Geographic locations of the study sites across Europe: Kärrbo Prästgård (Sweden), Jeggeleben (Germany), and Piacenza (Italy).

These locations were selected to capture diverse solar irradiation conditions. The data for those locations were retrieved from the ERA5 reanalysis dataset for the years 2018−2023. ERA5 provides hourly estimates of numerous climate variables on ~30 km grids globally [22]. For each location, hourly time-series of relevant weather variables including global horizontal irradiance (GHI), ambient temperature, wind speed, relative humidity, atmospheric pressure, and precipitation. Figure 3 presents a comparative analysis of key meteorological parameters (GHI, ambient temperature, relative humidity, and accumulated precipitation) across Sweden, Germany, and Italy.

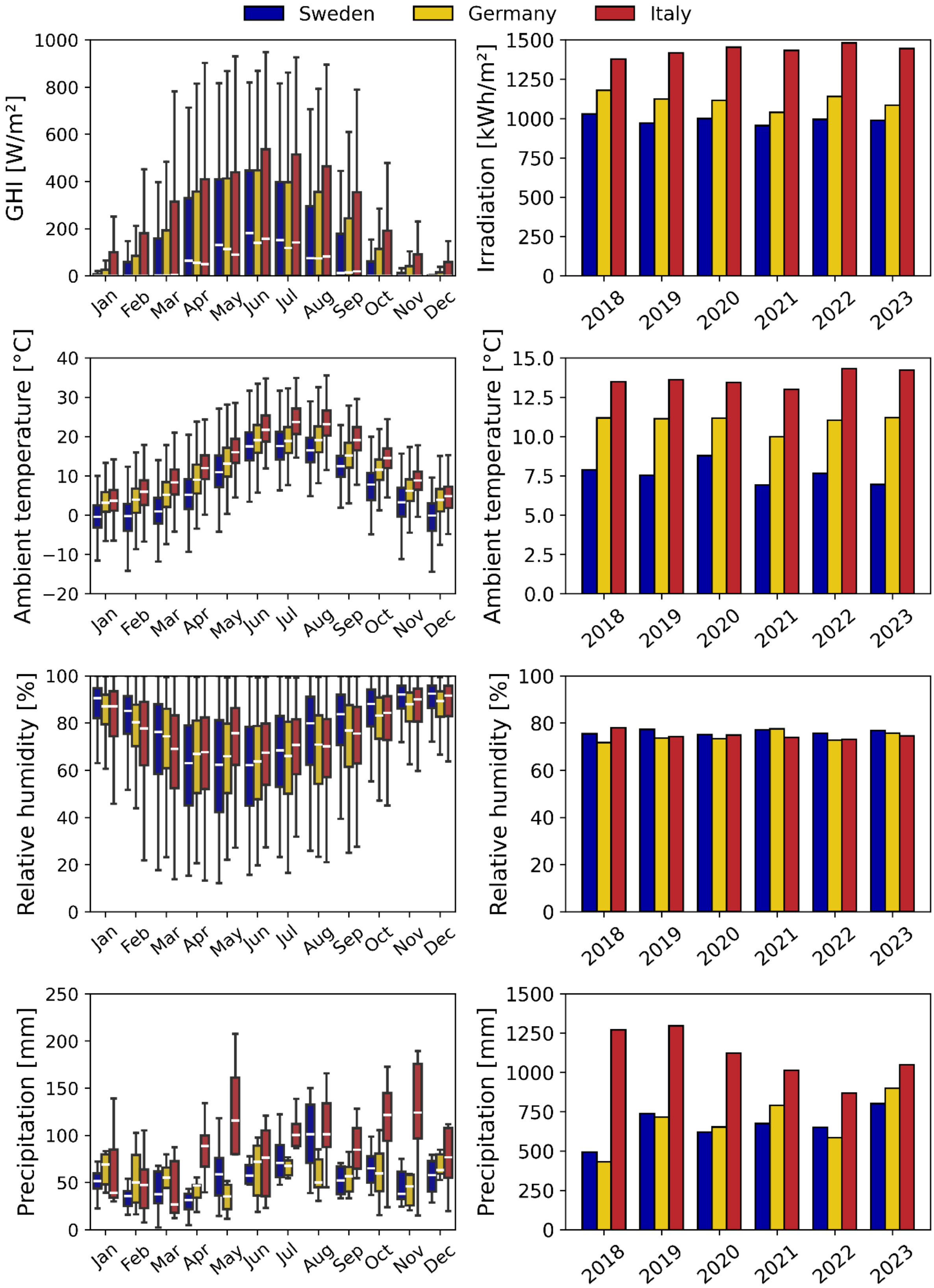

Figure 3. Weather variability across Sweden, Germany, and Italy within the period 2018−2023. The left column illustrates the seasonal distribution of these variables using boxplots, while the right column provides yearly averages from 2018 to 2023. Precipitation is shown as accumulated yearly totals rather than averages, allowing for the identification of extreme wet or dry periods.

A notable observation is the particularly dry condition in 2018 for Sweden and Germany, as indicated by both lower accumulated precipitation and reduced relative humidity during the summer months. In contrast, Italy does not exhibit the same reduction in precipitation, suggesting that the dry period was more regionally constrained to northern Europe as seen in Figure 3. Another feature is the significantly higher accumulated precipitation in Italy for 2019, which stands out compared to the more stable patterns observed in Sweden and Germany.

Prior to simulation, the ERA5 solar irradiance components were quality-checked by identifying anomalous values such as negative irradiance or unrealistic spikes, which were set to zero. Additionally, all irradiance values corresponding to solar elevation angle below 5° were also set to zero to avoid cosine-related artefacts commonly encountered at low sun angles [23]. The cleaned data were then converted into the input format by the Agri-OptiCE® model. In ERA5, the diffuse horizontal irradiance (DHI) is not available and was estimated using ERBS [24]. The ERBS model is commonly used to calculate the diffuse fraction from the GHI through an empirical relationship between diffuse fraction and the ratio of GHI to extraterrestrial irradiance. The crop model requires photosynthetically active radiation (PAR) as input, which was retrieved by assuming that 45% of the incoming GHI lies within the PAR spectrum [25]. Secondly, the diffuse PAR is required to accurately estimate the impact of both direct and diffuse components for the crop. The diffuse PAR were estimated using the GU model with the Spitters relationship [26].

All meteorological time series were gap-free and were formatted into annual input files for each site and year. The resulting dataset provides six years of continuous hourly climate inputs for each location, capturing interannual variability and seasonal patterns crucial for both PV performance and crop growth modelling.

2.2 Optimisation framework

The Agri-OptiCE® framework has been used as an integrated simulation and optimisation model custom-built for APV systems to evaluate and optimise system configurations. The framework extends a previously validated APV model [20,27–30] to incorporated additional design variables and performance metrics relevant to APV systems. It couples three primary sub-models: (1) a solar irradiance and shading model that computes the distribution of solar irradiance (including PAR) reaching both the PV modules and the crop, (2) a PV performance model for bifacial modules (accounting for front and rear irradiance, incidence angle effects, and temperature-dependent efficiency), and (3) a crop growth and yield model that responds to local climate and the microclimate modified by PV shading. These sub-models have been validated in earlier studies against field measurements and commercial PV software, demonstrating good agreement [20,27–30].

For PV simulations, a HUASUN Himalaya M6-144 bifacial heterojunction (HJT) solar module was used as the representative technology. This is a 144-cell, double-glass frameless module rated at approximately 480 W_p with an efficiency around 22.2% [31]. The module has dimensions of about 2.11 m × 1.04 m and a bifaciality factor (rear to front output ratio) of 95%. The electrical specifications can be seen in Table 1.

Table 1. PV module electrical characteristics (standard test conditions (STC)*).

Model	**HS-B144 (DNN480)**
Maximum power (P_{max})	480 W
Module Efficiency (%)	22.24 %
Optimum Operating Voltage (V_{mp})	46.08 V
Optimum Operating current (I_{mp})	10.43 A
Open Circuit Voltage (V_{oc})	53.74 V
Short Circuit Current (I_{sc})	10.82 A
Bifaciality	95 %
Nominal Operating Cell Temperature (NOCT)	44 °C
Temperature Coefficient of P_{max}	−0.26 %/°C
Temperature Coefficient of V_{oc}	−0.24 %/°C
Temperature Coefficient of I_{sc}	0.04 %/°C

*STC: Irradiance 1000 W/m^2, cell temperature 25 °C, AM=1.5. Tolerance of P_{max} is within +/− 3%.

The PV model calculates the instantaneous power from each module row, including the boost from rear-side irradiance due to ground reflection (albedo assumed to be 0.2). All simulations were conducted for a 1 ha plot (i.e., 100 m × 100 m).

2.3 Crop modelling and yield estimation

A uniform crop rotation sequence was considered at all three locations to evaluate APV performance under a variety of crop types and growth seasons. The rotation spanned six years (2018-2023) consisting of: ley grass for three consecutive years, followed by spring wheat (fourth year), barley (fifth year), and then returning to ley grass in the sixth year. In practice, “ley grass” refers to a perennial forage crop (e.g., alfalfa or grass-clover mix) which remains for multiple years once sown. By cycling through a multi-year grass period and annual cereals, the simulation captures both a crop that can benefit from partial shade (grass) and staple grain crops that are more light-demanding [32–35]. Each location applied the same rotation sequence, but with planting and harvest timings adjusted to local agronomic conditions.

The crop growth sub-model in Agri-OptiCE® is based on the EPIC model [36], which requires several inputs for each crop. We have chosen to use the pre-determined parameters that should be more generalised directly from EPIC for both barley and wheat [37]. However, for ley grass we have retrieved the inputs from previous research [28]. In all cases, the parameters reflect open-field conditions, without the influence of APV shading. The same crop parameters were assumed for all locations and can be found in Table 2.

Table 2. Crop parameters used for simulation.

	Ley grass	**Spring wheat**	**Barley**
Biomass–energy ratio* ((kg/ha)/(MJ/m^2))	24	30	30
Harvest index	0.7	0.42	0.4
Base temperature (°C)	0	0	0
Optimal temperature (°C)	14	15	15
Maximum leaf area index (LAI) (m^2/m^2)	5.5	5	6
Fraction of growing season when leaf area declines	0.85	0.6	0.8
LAI declining factor	0.5	1	1
Water stress-yield factor	0.21	0.21	0.21
First point on optimal leaf area development curve (%)	20	20.1	15.01
Second point on optimal leaf area development curve (%)	46	49.95	50.95

*Biomass-energy ratio is also known as radiation use efficiency (RUE).

Harvest dates were tailored to each crop and location. The ley grass, being perennial, is assumed to start regrowing after each harvest and continues until winter dormancy occurs, allowing multiple cuttings per year. We assumed three harvests per season for ley grass (e.g., early summer, midsummer, and early fall (Table 3) and one harvest per season for the annual crops (wheat, and barley, taken at full maturity). The model resets the crop each year according to the rotation schedule, but this applies only to barley and wheat, not to ley grass. Crop phenology (development stages) is driven by accumulated growing degree-days with base temperature of 0 °C for these crops. Water balance is also tracked: soil moisture availability and evapotranspiration (ET) affect growth via a water stress factor; however, all the crop simulations were conducted under rainfed conditions, with no supplemental irrigation assumed beyond natural rainfall. Even though wheat and barley are generally not irrigated, the reduced

ET under panels can still illustrate potential water-saving benefits, particularly when compared to full-sun conditions.

Table 3. Cut dates by crop and country based on regional agricultural calendars.

Crop	**Country**	**Cut 1**	**Cut 2**	**Cut 3**
Ley grass	Sweden	June 1	July 20	September 17
	Germany	May 22	July 21	September 21
	Italy	May 15	July 10	September 10
Spring wheat	Sweden	June 30		
	Germany	August 30		
	Italy	July 15		
Barley	Sweden	June 30		
	Germany	August 30		
	Italy	July 15		

Crop yields (tons per hectare) are computed at each harvest using the accumulated biomass and the crop's harvest index. For ley grass, yields from each of the three cuts are summed for an annual total yield. The presence of PV rows can reduce incoming PAR on the crops and thereby reduce growth. Moreover, the area immediately beneath the PV rows is considered non-productive, as crops are not planted or harvested there due to limited machinery access and deep shading that inhibits growth. To reflect this, a buffer zone of 0.5 meters on each side of the PV rows is assumed to be non-harvestable. These areas are excluded from yield calculations to account for safety margins and technical constraints related to mechanised operations, such as the limited height of the modules and structural obstructions that prevent cultivation directly beneath them. The extent of land loss in percentage varies with system design, with narrow-pitch APV configurations exhibiting the highest proportion of non-cropped surface [38]. Accordingly, buffer zones were considered for each system layout, and the corresponding strips were excluded from the calculation of fresh yield under APV conditions.

2.4 Performance metrics calculation

To quantify the performance of each APV configuration, a set of WEF metrics at the end of each optimisation iteration is used to evaluate the APV system. It includes:

- **LER:** This metric measures the land-use efficiency of the APV system, combining relative crop yield and relative PV output. It is defined as:

$$LER = \left(\frac{Y_{c,APV} \cdot \chi}{Y_{c,ref}}\right) + \left(\frac{Y_{e,APV}}{Y_{e,ref}}\right) = LER_{crop} + LER_{PV}, \quad (1)$$

where $Y_{c,APV}$ is the crop yield (ton ha^{-1}) under the APV system and $Y_{c,ref}$ is the yield in the reference scenario without PV (open-field), while $Y_{e,APV}$ is the annual PV electricity yield per unit land area (kWh ha^{-1} or equivalently kWh m^{-2} over the field) and $Y_{e,ref}$ is the corresponding electricity yield if the entire land were used for a stand-alone PV park. χ is the reduction factor considering the land loss close to the mounting structure that cannot be harvested. The reduction factor can be calculated by $1 - \frac{b}{a}$, where b represents the width of the buffer zones that is designated as non-harvestable. This width is assumed to be 1 m (0.5 m on each side of the mounting structure). The non-harvestable area is divided by the pitch, denoted as a.

- **Water consumption:** The total crop water use in each scenario is tracked via modelled ET. The cumulative seasonal ET (mm of water evaporated + transpired) serves as an indicator of water consumption by crops. In APV systems, shading can reduce soil evaporation and plant transpiration during hot periods, potentially yielding water savings. In this study, we assess water consumption by comparing the cumulative ET under APV conditions to that under open-field conditions. This relative measure is used as a proxy for potential water savings, under the assumption that rainfall is the only source of moisture and that any reduction in ET corresponds directly to reduced water use by crops. We do not model irrigation or refer to water reintegration percentages commonly used in irrigation studies.

All metrics were computed on an annual basis for each year and then averaged over the rotation cycle for final evaluation, to smooth out year-specific weather anomalies.

2.5 Regulatory and policy constraints

The integration of PV systems with agricultural activity presents regulatory challenges that vary across national contexts. To ensure that APV installations align with agricultural and energy policy objectives, several countries have established thresholds for light availability, land occupation, and crop yield retention. In this study, APV designs are evaluated based on three regulatory frameworks: the Swedish basic payment scheme (BPS) requirements, German crop yield retention guidelines, and Italian APV best practices.

2.5.1 Swedish BPS compliance (C1)

In Sweden, agricultural subsidies under the BPS impose restrictions on PV installations to ensure that farming remains the primary land use. According to the Swedish Board of Agriculture (*Jordbruksverket*), land covered by PV structures is generally ineligible for subsidies unless agricultural activity is not significantly impaired [39]. It is important to note that this is not an APV regulation, law, or standard, but rather a condition for receiving agricultural subsidies. The eligibility assessment is based on whether mechanised farming can continue unhindered, and a maximum of 10% of the land area may be occupied by solar infrastructure for the installation to remain subsidy-eligible.

2.5.2 Germany crop yield retention guidelines (C2)

Germany's APV framework is guided by the technical pre-standard DIN SPEC 91434:2021-05, which outlines design principles to ensure that agricultural production remains the primary land use [40]. While this specification is not legally binding, it is widely recognised and increasingly referenced in federal policy, subsidy frameworks, and funding programs.

According to DIN SPEC 91434, APV systems should:

- Maintain at least 66% of the baseline open-field crop yield, compared to reference values from conventional agriculture.
- Limit permanent land occupation by PV structures based on system configuration:
  - Spaced APV systems (e.g., inter-row installations): maximum 15% land loss.
  - Overhead APV systems (e.g., elevated to allow full machinery access): maximum 10% land loss.

The 66% crop yield retention is a recommended performance benchmark, not a legal requirement. It serves as a key indicator of agronomic viability and is often used in feasibility studies and project evaluations, particularly for pilot or publicly funded projects. The land occupation thresholds, however, have been partially codified into national regulation. Under Germany's common agricultural policy (CAP) implementation [41], the direct payments ordinance (GAP-Direktzahlungen-Verordnung) states that APV systems may still receive area-based subsidies, such as basic income support, only if they preserve agricultural use and limit land loss to no more than 15%. This approach ensures that APV projects do not compromise eligibility for CAP subsidies. This mechanism is comparable to Sweden's BPS, where land equipped with solar panels can remain eligible for direct payments provided that agricultural activity continues, and the installation does not significantly hinder normal farming practices. Additionally, APV systems in Germany participating in renewable energy auctions under the renewable energy act (EEG) 2023 must comply with criteria aligned with DIN SPEC 91434, including land-use limits [42]. Overhead systems that meet the 10% ground coverage limit and allow full machinery operation are also eligible for a tariff bonus through the federal network agency (BNetzA), incentivising designs that minimise land occupation.

2.5.3 Italian guidelines for APV (C3)

Italy has adopted a multi-threshold regulatory framework for APV systems to ensure a balanced integration of energy conversion and agricultural activity [43,44]. This framework, formalised in the Ministerial Decree 2023 [45], defines the legal requirements for APV systems seeking public incentives and includes the following criteria:

1. At least 70% of the project area must remain available for agricultural use, effectively limiting the maximum land occupation by PV infrastructure to 30%. This ensures that the system maintains its agricultural function and avoids excessive land loss to energy infrastructure.
2. The APV system must produce at least 60% of the annual electricity output of a conventional ground-mounted PV installation. This requirement guarantees a minimum level of solar conversion efficiency, even in spatially dispersed APV layouts.
3. PV modules must be elevated from the ground to allow continued agricultural operations. The legally required minimum height is 2.1m for crop cultivation systems and 1.3m for livestock or pasture-based systems, ensuring compatibility with machinery or grazing activity.

These thresholds were initially proposed in national technical guidelines and have now been codified into national legislation for all APV projects participating in publicly funded support schemes. Additionally, the 2023 national best practices (UNI/PdR 148:2023 [46]) recommend that agricultural productivity under APV systems should not decline by more than 30% per hectare compared to conventional farming. While this remains a non-binding recommendation, it has become an evaluation metric, especially through the productivity land value (PLV) methodology. PLV assessments are required for incentive eligibility and are used to demonstrate that APV systems do not significantly impair agricultural output, thus making the yield loss recommendation a *de facto* requirement in practice. To verify the 60% electricity production threshold, the national guidelines use example simulations modelled with PVGIS. These simulations apply a bifacial correction factor and assume a ground coverage ratio (GCR) of 0.49 for the reference conventional PV system.

In contrast, this study applies a different methodology to ensure consistency across systems and better capture APV interactions. We use Agri-OptiCE®, which incorporates the bifacial nature of the modules directly. It is also assumed that the reference conventional PV system has a GCR of 0.416, which represents a slightly more spaced layout as used in the guidelines to keep it consistent between all locations and system simulated. In this study, we chose to combine the legally binding requirements outlined in the national legislation with the technical recommendations provided in the 2023 national APV best practices. This integrated approach allows us to evaluate and identify optimal APV system configurations that not only comply with regulatory thresholds for land use, energy conversion, and module elevation, but also aim to maintain agricultural productivity within acceptable limits.

2.5.4 Implementation and design considerations

Given these regulatory constraints, APV system design must be adapted to comply with different national requirements. Systems that exceed permissible land occupation, reduce crop yields below mandated levels, or fail to meet solar electricity production targets are considered non-viable within their respective frameworks. These key policy constraints across Sweden, Germany, and Italy are summarised in Table 4. This study evaluates APV configurations against these policy constraints to determine optimal designs that balance agricultural productivity and energy conversion. The Swedish BPS compliance, Germany crop yield retention standards, and Italian best practices for APV will be referred to as C1, C2, and C3, respectively, throughout the study.

Table 4. National policy constraints guiding APV system design for Sweden, Germany, and Italy.

Constraint	C1	C2	C3
Max. land occupation	⩽ 10% of land area for solar infrastructure	⩽ 15% for spaced systems ⩽ 10% for overhead systems (to qualify for tariff bonus)	⩽ 30% of project area (i.e., 70% ⩾ must remain available for agriculture)
Minimum crop yield retention	Not specified (farming must not be “significantly impaired”)	⩾ 66% of open-field reference yield (recommended benchmark, used in funding and feasibility)	⩽ 30% yield loss per hectare compared to conventional farming (non-binding, but indirectly used in incentive evaluations via PLV)
Minimum solar production	Not specified	Not specified	⩾ 60% of the annual electricity output of a conventional ground-mounted PV system

Elevation requirement	Not specified (only that mechanised farming must not be hindered)	Overhead systems must allow full machinery access	⩾ 2.1 for crops ⩾ 1.3m for livestock/pasture

2.6 Water-energy-food nexus index

To encapsulate the triple bottom line of APV performance (water use, energy conversion, and food production), a composite WEF nexus index, as proposed by El-Gafy [47], was adopted as a single optimisation criterion. This index allows for a multi-objective representation of the three competing criteria and serves as an aggregated performance measure within an optimisation framework. A critical aspect of constructing such an index is ensuring that all contributing metrics: water use, energy conversion efficiency, and food production are equitably represented, particularly when their numerical scales differ significantly. To address this challenge, a Utopia-Nadir normalisation approach is applied to remove scaling biases, followed by an adaptive weighted sum strategy to improve Pareto front exploration. The WEF nexus index is constructed as a weighted sum of normalised objectives, ensuring a balanced representation of water efficiency, energy conversion (LER_{PV}), and food production (LER_{crop}). The general weighted sum formulation for a multi-objective optimisation problem is:

$$J_{\text{total}} = \sum_{i=i}^{m} w_i J_i^* , \tag{2}$$

where J_i^* represents the normalised performance score of the ith objective, and w_i is the weighting coefficient that determines its relative importance. The weights must satisfy:

$$\sum_{i=i}^{m} w_i = 1 , \qquad w_i \geq 0 \tag{3}$$

Applying this to the WEF index, the total performance score is expressed as:

$$\mathcal{W} = w_w \cdot W^* + w_e \cdot E^* + w_f \cdot F^*, \tag{4}$$

where W^*, E^*, and F^* are the normalised objectives for water use, energy conversion efficiency (LER_{PV}), and food production (LER_{crop}), respectively. In the baseline scenario, each component is given equal priority, resulting in:

$$w_w = w_e = w_f = \frac{1}{3} \tag{5}$$

This formulation ensures that all three objectives contribute equally, preventing any single factor from dominating the optimisation process. The weighting scheme can be adjusted to reflect context-specific priorities. For instance, if the analysis focuses on a water-scarce region, the weight assigned to water efficiency should be greater than those for energy and food, i.e., $w_w > w_e$ and $w_w > w_f$. In contrast, when food security is the dominant concern, the weight on food production can be prioritised, such that $w_f > w_w$ and $w_f > w_w$. Similarly, if the main objective is to maximise renewable energy output, the emphasis can shift towards energy conversion efficiency, with $w_e > w_w$ and $w_e > w_f$. This dynamic weighting mechanism enables decision-makers to tailor the optimisation process to align with specific sustainability objectives, ensuring that APV systems are optimised according to local needs. A fundamental challenge in multi-objective optimisation is ensuring that all objectives contribute equitably, irrespective of their numerical magnitudes. Without proper normalisation, objectives with larger inherent values may dominate the optimisation process, leading to biased solutions. To mitigate this issue, each performance metric is normalised using the Utopia and Nadir points, which define the best and worst observed values among Pareto-optimal solutions. In Figure 4, a representation of how the points are considered for two objectives is shown.

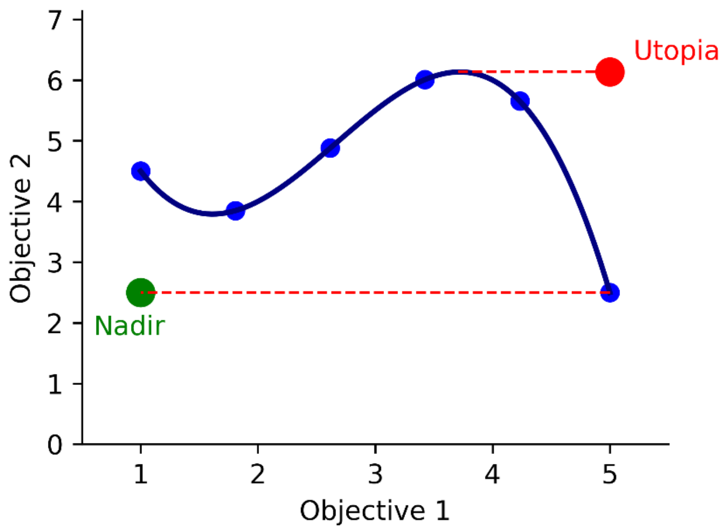

Figure 4. Conceptual illustration of a Pareto front in a two-objective maximisation problem, with corresponding Utopia (red) and Nadir (green) points. The Utopia point represents the ideal solution, where both objectives achieve their highest possible values. The Nadir point reflects the worst performance across the Pareto-optimal set.

The plot illustrates the relative positioning of the Nadir and Utopia points in the context of the two objectives, highlighting the trade-offs between them. For an objective function J_i, its normalised value J_i^* is given by:

$$J_i^* = \frac{J_i - J_{i,U}}{J_{i,N} - J_{i,U}}, \tag{6}$$

where $J_{i,U}$ represents the Utopia point, which is the most favourable value achievable for that objective in isolation and $J_{i,N}$ represents the Nadir point, which corresponds to the least favourable value observed among the Pareto-optimal solutions. For an objective function $J_i(x)$, the Utopia point is given by:

$$\begin{aligned} J_{i,U} &= \min_{x \in \mathcal{F}} J_i(x), \qquad \text{for minimisation} \\ J_{i,U} &= \max_{x \in \mathcal{F}} J_i(x), \qquad \text{for maximisation} \end{aligned} \tag{7}$$

where $\mathcal{F}$ represents the entire feasible solution space, including both dominated and non-dominated solutions. Similarly, for an objective function $J_i(x)$, the Nadir point is given by:

$$\begin{aligned} J_{i,N} &= \min_{x \in \mathcal{P}} J_i(x), \qquad \text{for minimisation} \\ J_{i,N} &= \max_{x \in \mathcal{P}} J_i(x), \qquad \text{for maximisation} \end{aligned} \tag{8}$$

where $\mathcal{P}$ is the Pareto-optimal set, meaning it only contains solutions that are not dominated by any other feasible solution. This normalisation ensures that each objective is mapped to the range $[0,1]$, preventing any single metric from dominating the optimisation process. The proposed WEF index, combined with Utopia-Nadir normalisation and an adaptive weighted sum approach, offers several key advantages. Firstly, bias-free scaling ensures that the optimisation process does not favour objectives with naturally larger numerical values. Secondly, adaptive weighting improves solution diversity, leading to a more representative Pareto front. Thirdly, the flexibility of the approach allows decision-makers to dynamically adjust the relative importance of water, energy, and food metrics based on context-specific needs.

2.7 Optimisation methodology

In this study, an optimisation approach is employed to explore combinations of key design parameters, such as PV orientation, mounting height, row spacing, and system design (vertical, one-axis tracking, or overhead). This enables the identification of the most suitable configuration for a given location, based on predefined performance objectives. GA was chosen to perform this optimisation. GA is well-suited for exploring large design spaces with complex trade-offs, and they do not require gradient information. The chosen parameter space for these parameters were defined as (orientation $\in$ [−180°, 180°] with a step of 15°, height $\in$ [0.5, 2] m for vertical, [3, 3.5] m for overhead, and [1.5, 3.5] m for trackers, all with a step of 0.5 m, and pitch $\in$ [5, 20] m with a step of 1 m).

The GA optimisations were performed using a population size of 200 and 200 generations, which was sufficient for the fitness values to converge to stable levels. The crossover and mutation probabilities were set to 80% and 20%, respectively, consistent with values reported in recent literature for maintaining a balance between exploration and exploitation in GA [48]. Similar metaheuristic approaches, such as differential evolution, have also been successfully applied to PV parameter optimisation problems, highlighting the robustness of evolutionary techniques for nonlinear and multi-dimensional design spaces [49]. The performance of the GA was evaluated based on the progression of this composite WEF index, as shown in Figure 5, which illustrates the convergence behaviour of both the best and average fitness values across generations.

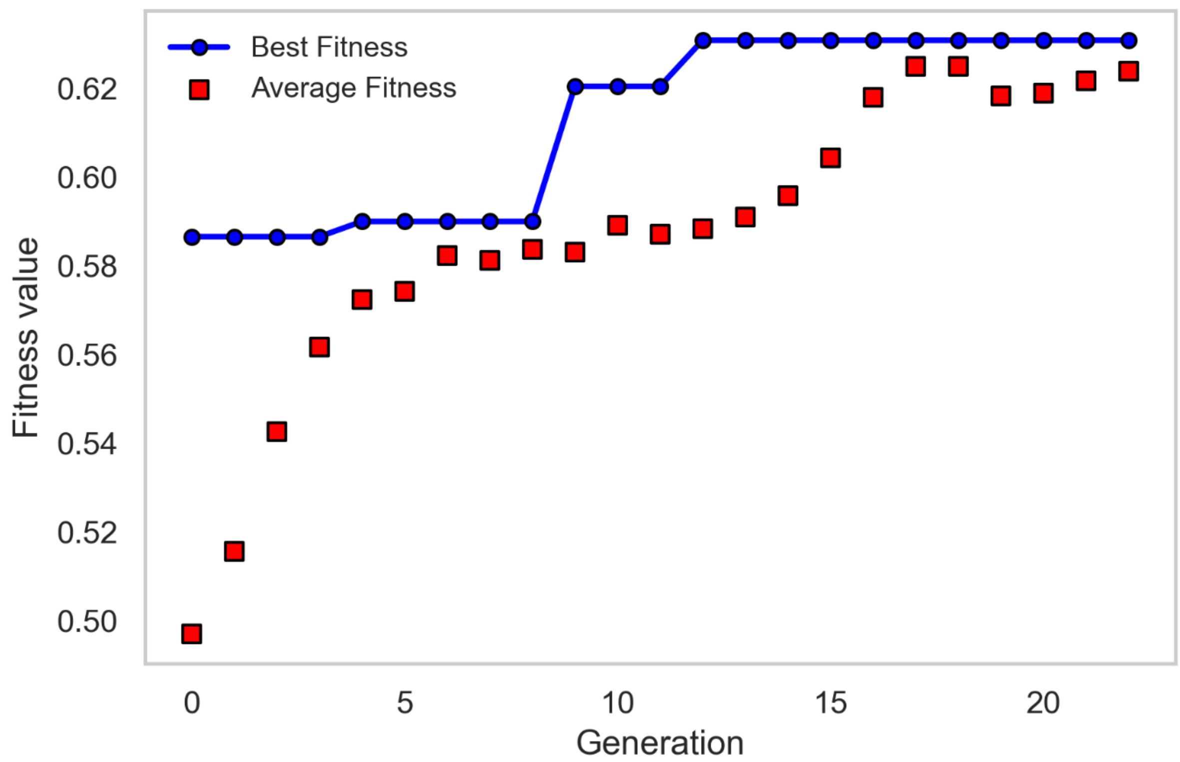

Figure 5. Fitness evolution of the WEF index objective function using a GA. The plot shows the progression of the best fitness (blue line) and average fitness (red squares) over generations, demonstrating convergence towards an optimal solution.

The convergence simulation terminates early if no improvement is observed over 10 consecutive generations. From these trials, it is evident that a population size of 200 with 50 generations is sufficient to find an optimal design for all objective functions and will therefore be used in the GA. The GA process was repeated for each site. To further ensure that the identified solutions are indeed optimal, a local exhaustive search using a refined GA was performed in the neighbourhood of the converged design points.

2.8 Scenario definitions

To investigate how differing sustainability and economic goals influence system performance, we define four scenarios.

2.8.1 WEF scenario

This scenario represents a balanced sustainability strategy, assigning equal weight to each of the three environmental indicators $w_w = \frac{1}{3}$, $w_e = \frac{1}{3}$, and $w_f = \frac{1}{3}$. It reflects contexts where trade-offs among water use, food security, and renewable energy are all critical, such as arid and semi-arid regions with national sustainability targets.

2.8.2 Energy food (EF) scenario

In the EF scenario, water is excluded from the objective function $w_w = 0$, $w_e = \frac{1}{2}$, and $w_f = \frac{1}{2}$. This scenario is relevant in regions or applications where water is not a constraining factor, either due to irrigation technologies, abundant availability, or policy preferences focused on food and energy production.

2.8.3 Water-energy-economy-food (WEEF) scenario

Although WEF-optimised designs may appear sustainable, they might not be economically viable. Therefore, we include a WEEF scenario $w_w = \frac{1}{4}$, $w_e = \frac{1}{4}$, $w_{ec} = \frac{1}{4}$, and $w_f = \frac{1}{4}$, which extends the WEF framework by integrating net present value (NPV) as an indicator of long-term economic feasibility. Where w_{ec} is the weight added to the WEF objective function to consider the economic viability. The NPV is calculated over a 30-year system lifetime using the standard discounted cash flow formula:

$$NPV = -ICC + \sum_{t=1}^{n} \frac{CF_{in,t} - CF_{out,t}}{(1 + WACC)^t}, \tag{9}$$

where ICC is initial capital cost, $CF_{in,t}$ is the cash inflows (crop revenue, electricity income, subsidies), $CF_{out,t}$ is the operations and maintenance costs and inverter replacement, $WACC$ is the real weighted average cost of capital, and n is the system lifetime. The economic evaluation is based on techno-economic parameters for Sweden, Germany, and Italy from Zidane et al. [50] and is presented in

Table 5. The 6-year crop rotation are repeated five times to model a full 30-year lifecycle.

Table 5. Economic assumptions use in NPV calculations.

Parameter	**Sweden**	**Germany**	**Italy**
Crop producer price (€/ton)	[111, 197, 189]	[111, 210, 194]	[111, 293, 194]
[Ley grass, spring wheat, barley]			
Crop producer cost (€/ton)	[128, 113, 138]	[128, 113, 138]	[128, 113, 138]
[Ley grass, spring wheat, barley]			
Electricity price (€/kWh)	0.08707	0.1116	0.14485
Subsidy (€/ha/year)	232	286	343
CAPEX per kWp	[1001, 1009, 1217]	[1001, 1009, 1217]	[1001, 1009, 1217]
[Vertical, one-axis, overhead]			
Operation & maintenance cost	1% of CAPEX annually	1% of CAPEX annually	1% of CAPEX annually
Inverter replacement (Year 17)	55 €/kWp	55 €/kWp	55 €/kWp
System lifetime	30 years	30 years	30 years
WACC	3.5%	3.5%	3.5%

2.8.4 WEF boosted (WEFb)

Crop models are typically calibrated for open-field monocultures under full sun and therefore do not capture beneficial physiological responses to partial shading [51,52]. Since they are parameterised for open-field conditions, they overlook shade-induced effects such as changes in canopy morphology and light-use efficiency [12]. To test whether such responses could alter the outcome, the maximum LAI and RUE values were increased by 20% for each crop to represent the potential morphological effects of partial shading. This adjustment is supported by a growing body of field-based evidence showing that shading, whether from intercropping, agroforestry, or structural elements, can enhance RUE and LAI through mechanisms such as increased nitrogen availability, improved canopy light distribution, and morphological acclimations [53–56], it does not represent a calibrated or universal value. The actual magnitude of these responses may vary significantly across environments, cultivars, and shading conditions. Rather, this sensitivity test is intended to explore the potential significance of such effects in APV systems. To capture these effects, we introduce a sensitivity scenario where maximum LAI and RUE are increased by 20% for all crops. The weights used under this scenarios is $w_w = \frac{1}{3}$, $w_e = \frac{1}{3}$, and $w_f = \frac{1}{3}$.

2.9 Sensitivity analysis of design parameters

To better visualise the optimisation process, a comprehensive sensitivity analysis was conducted to explore the APV design space and assess the impact of key system configuration parameters. The factors and ranges analysed were as follows:

- **PV row orientation:** The azimuthal orientation of the PV rows (the direction the module surface normal faces) was varied from −180° to 180°. This range spawns all possible alignments, with 0° representing a south-facing orientation (in the Northern Hemisphere). Positive angles indicate a clockwise rotation from south, so 90° corresponds to west-facing panels, while negative angles indicate a counterclockwise rotation, so −90° corresponds to east-facing panels. For vertical bifacial panels, this means one side faces east (−90°) and the other side faces west (90°).
- **PV height:** The height of the PV module above ground was tested from 1.5 m up to 3.5 m for one-axis tracker configurations (defined as the height of the tracker axis), and from 0.5 m up to 2.0 m for vertical fixed panels. Lastly, the overhead configuration is assumed to only be 3 m up to 3.5m. For the vertical and overhead configurations, height is defined as the distance from the ground to the lowest edge of the PV module.
- **Row pitch:** The APV systems pitch varied from 5 m (very dense packing) to 20 m (sparse rows). This pitch distance directly influences the GCR and thus the fraction of land receiving shade. A 5 m spacing implies about 20 rows per 100 m field width, whereas a 20 m spacing has only 5 rows across the field.
- **Tilt:** For the vertical APV system, the tilt angle was fixed at 90°. The tracking system had a maximum tilt angle of 60°, as this is a common limit in modern APV systems [57]. Lastly, the overhead system was assumed to have a fixed tilt angle of 35°.

All APV systems in the study used the same layout: PV modules were arranged in a two-module landscape format per row (i.e., each row hold 2 modules side-by-side in landscape orientation). Throughout the simulation, the ground surface albedo was kept constant at 0.2 to focus the results on geometric effects rather than surface reflectivity. The performance of the APV systems was compared to two references cases: (1) open-field (full sun) conditions for crop yield, and (2) a conventional PV park design for energy conversion, which used a pitch of 5 m, height of 0.5 m, and a PV module tilt of 35°. The conventional PV layout also used 2 modules in landscape orientation per row.

3 Results

3.1 Correlation and optimal parameters

The choice of weighting for water, energy, economy, and food significantly influences the optimal APV system configuration. It could be observed that all scenarios found different optimal system designs. Additionally, regulatory constraints play a crucial role in defining the feasibility of each system.

Table 6 presents the optimal row pitch, height, PV orientation, and system configuration for the three investigated locations under different policy or guideline-driven constraints. The values shown for LER, LER_{crop}, LER_{PV}, and water consumption represents the average annual performance across the entire six-year simulation period, incorporating the full crop rotation sequence (three years of ley grass, followed by spring wheat, barley, and one final year of ley grass). This means that crop-related metrics (yield and water consumption) reflect the rotation-averaged performance, not individual crop-year values. A key finding is that the Italian constraint (C3) is infeasible across all scenarios except WEFb, indicating that no configuration met the required constraints in any of the studied regions. The WEFb-scenario allowed configurations to achieve a significant improvement in system performance, with the LER values increasing and water consumption decreasing compared to the WEF-scenario

Interestingly, the optimal PV orientation rarely followed conventional designs. Under the WEF-scenario, a one-axis tracker with a $-60°$ southeast deviation emerged as the optimal configuration in Sweden's subsidy-based constraint setting (C1). While this setup slightly reduces PV production compared to an east-west ($-90°$) tracker, it enhances crop yield, making it the most balanced choice in terms of LER. Comparing C1 and the German standard constraints (C2), the less restrictive land-use constraints in C2 resulted in a reduced row pitch, allowing for higher PV capacity. However, meeting the crop yield constraint necessitated the adoption of overhead system for all three countries. Notably, the optimal PV orientation in C2 deviated from the common south oriented fixed tilted systems, shifting to satisfy the crop yield constraint while minimising row pitch. In addition to this, a clear latitudinal trend emerged, at lower latitudes with higher solar irradiance, the optimal PV orientation shifted closer to south-facing configurations. In Italy, for instance, the overhead system performed best with a $-15°$ PV orientation, as this orientation allowed the crop yield constraint in C2 to be satisfied while also enhancing PV electricity production.

Table 6. Optimal APV system configurations for each location under different constraint scenarios.

Scenario	**Location**	**Row pitch (m)**	**Height (m)**	**PV orien-tation (°)**	**System solution**	**LER_{crop}**	**LER_{PV}**	**LER**	**WC* (%)**	**NPV (k€)**
WEF	Sweden (C1)	10.0	3.5	−60	One-axis	0.69	0.56	1.25	90.5	506
	Germany (C1)	10.0	3.5	−75	One-axis	0.70	0.54	1.25	90.6	889
	Italy (C1)	10.0	3.5	−75	One-axis	0.73	0.54	1.27	86.4	1810
	Sweden (C2)	7.0	3.0	−90	Overhead	0.66	0.60	1.26	89.0	198
	Germany (C2)	7.0	3.0	−75	Overhead	0.66	0.62	1.29	88.7	725
	Italy (C2)	7.0	3.0	−15	Overhead	0.67	0.69	1.36	83.4	2090
	Sweden (C3)	N/A	N/A	N/A	N/A	N/A	N/A	N/A	N/A	N/A
	Germany (C3)	N/A	N/A	N/A	N/A	N/A	N/A	N/A	N/A	N/A
	Italy (C3)	N/A	N/A	N/A	N/A	N/A	N/A	N/A	N/A	N/A
Scenario										
EF	Sweden (C1)	10.0	1.5	0	One-axis	0.72	0.54	1.26	91.4	464
	Germany (C1)	10.0	0.5	0	Vertical	0.79	0.43	1.21	94.0	575
	Italy (C1)	10.0	3.0	0	Overhead	0.77	0.50	1.26	88.3	1502
	Sweden (C2)	7.0	0.5	−180	Vertical	0.69	0.62	1.31	91.1	391
	Germany (C2)	7.0	0.5	0	Vertical	0.70	0.59	1.29	91.7	787
	Italy (C2)	7.0	3.0	0	Overhead	0.67	0.69	1.36	83.4	2099
	Sweden (C3)	N/A	N/A	N/A	N/A	N/A	N/A	N/A	N/A	N/A
	Germany (C3)	N/A	N/A	N/A	N/A	N/A	N/A	N/A	N/A	N/A
	Italy (C3)	N/A	N/A	N/A	N/A	N/A	N/A	N/A	N/A	N/A
Scenario										
WEEF	Sweden (C1)	10.0	3.5	−75	One-axis	0.69	0.56	1.25	90.4	507
	Germany (C1)	10.0	3.5	−75	One-axis	0.70	0.54	1.25	90.6	889
	Italy (C1)	10.0	3.5	−75	One-axis	0.73	0.54	1.27	86.4	1810
	Sweden (C2)	9.0	3.5	−45	One-axis	0.67	0.61	1.28	89.7	545
	Germany (C2)	8.0	3.5	0	One-axis	0.66	0.63	1.29	89.3	1003
	Italy (C2)	7.0	3.0	0	Overhead	0.67	0.69	1.36	83.4	2099
	Sweden (C3)	N/A	N/A	N/A	N/A	N/A	N/A	N/A	N/A	N/A
	Germany (C3)	N/A	N/A	N/A	N/A	N/A	N/A	N/A	N/A	N/A
	Italy (C3)	N/A	N/A	N/A	N/A	N/A	N/A	N/A	N/A	N/A
Scenario										
WEFb	Sweden (C1)	10.0	3.5	−60	One-axis	0.83	0.56	1.40	92.1	506
	Germany (C1)	10.0	3.0	−15	Overhead	0.91	0.5	1.41	93.3	663
	Italy (C1)	10.0	3.5	−75	One-axis	0.90	0.54	1.44	88.2	1810
	Sweden (C2)	7.0	3.5	−60	One-axis	0.69	0.77	1.46	88.1	682
	Germany (C2)	7.0	3.0	−15	Overhead	0.78	0.70	1.48	89.7	923
	Italy (C2)	7.0	3.5	−75	One-axis	0.76	0.75	1.51	82.3	2491
	Sweden (C3)	5.0	0.5	−180	Vertical	0.71	0.88	1.59	89.6	552
	Germany (C3)	5.0	3.0	−105	Overhead	0.71	0.79	1.50	87.0	752
	Italy (C3)	5.0	3.0	−75	Overhead	0.70	0.86	1.56	79.4	2422

Water consumption

In the WEEF-scenario, where economic performance was included in the objective function, the optimisation favoured designs that balanced financial return with resource efficiency, often leading to increased row pitches and a shift from overhead to one-axis tracking systems compared to WEF. This allowed for higher PV output and revenue while still satisfying crop yield constraints, resulting in significantly higher NPV values, for example, in Sweden (C2), NPV increased from €198k (WEF) to €545k (WEEF). In contrast, the WEFb-scenario revealed how improved crop responsiveness to partial shading shifted the optimisation towards food-prioritised layouts. The LER_{crop} increased across all sites, and new optimal configurations emerged, leading to overall LER values exceeding 1.5 in some cases. These results highlights the sensitivity of optimal APV designs to both economic assumptions and crop model parameters. In the EF-scenario, where water was excluded, APV configurations changed significantly. In this case, maximising crop yield became a more influential factor, leading to vertical APV systems beginning to become an optimal solution. As water consumption decreases with a lower row pitch, similar to how electricity production increases with a lower row pitch due to higher installed capacity per hectare, removing water consumption from the objective function allowed crop yield to have a stronger influence on the system design. This shift made crop yield a more prominent consideration in the design process for some solutions, compared to the previous scenario. Interestingly, the optimal PV orientation was not the east-west (−90°) for the vertical APV system but instead faced north-south (0°). This orientation reduces the incidence angle between the PV modules and the sun throughout the day, increasing ground irradiance and enabling a further reduction in row pitch, ultimately leading to an increased LER. To substantiate the relationship between module orientation and ground-level PAR availability, simulations were conducted using full datasets from 2018−2023. Figure 6 shows the average angle of incidence (AOI) between incoming sunlight and PV modules during each crop season, alongside the corresponding seasonal average PAR reduction for various system configurations. In Figure 6, the analysis is based on averages taken over the crop growing season for each year, reflecting the periods most relevant for APV performance. A consistent trend is observed were configurations with lower AOI exhibit higher PAR reduction, as more sunlight is intercepted by the PV modules and less reaches the ground. Conversely, higher average AOI leads to lower PAR reduction, allowing more irradiance to reach the area beneath the array. This inverse relationship between AOI and ground-level PAR is evident across all system types and locations, supporting the conclusion that the AOI plays a key role in determining under-panel light conditions. These results have been further validated by comparison with simulations from bifacial_radiance [58], as shown in the Appendix, which confirms the accuracy of our estimates and the robustness of the observed trends.

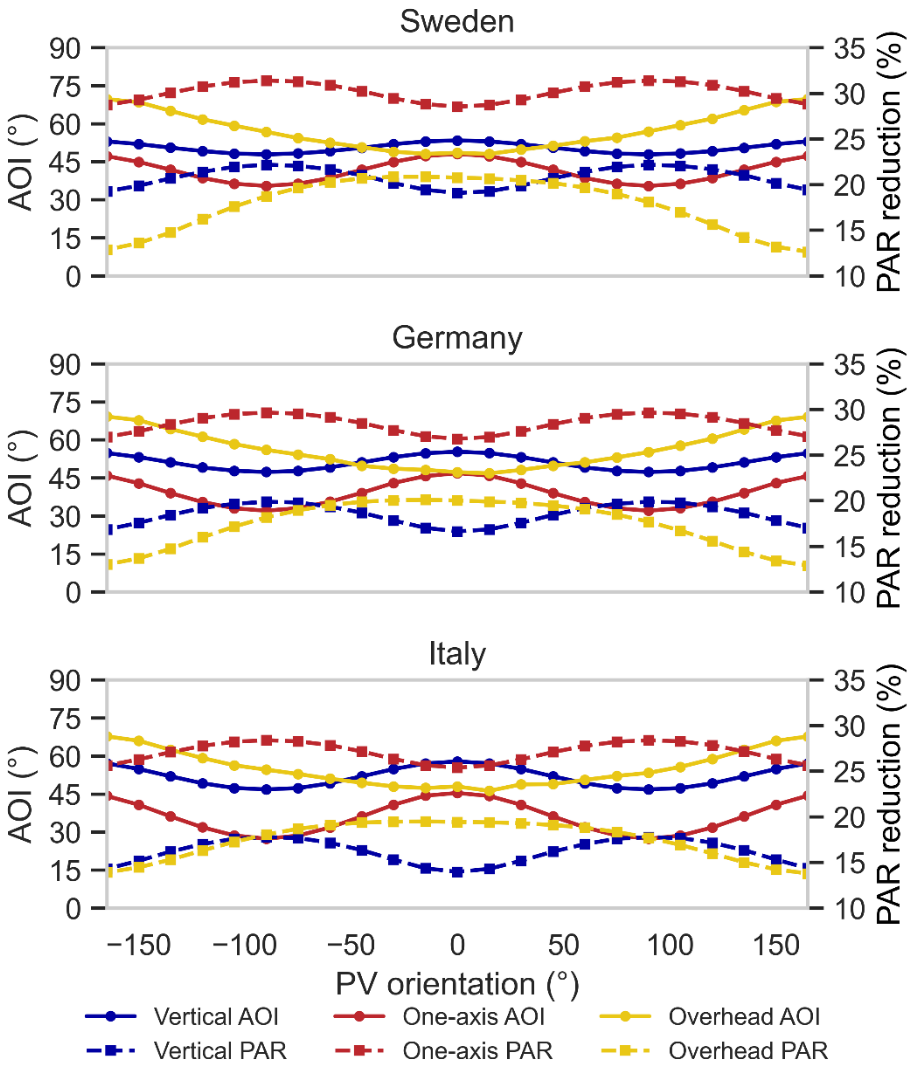

Figure 6. Seasonal average AOI (solid lines) and corresponding seasonal average ground-level PAR reduction (dashed lines) as a function of PV module orientation for three system configurations: vertical (0.5 m module height), one-axis tracking (2 m axis height), and overhead (3 m mounting height), all with a row pitch of 10 m. Data represent averages taken over the crop growing season for each year from 2018 to 2023, reflecting periods most relevant for APV system performance.

To better understand the influence of each parameter on the respective KPIs, the correlation analysis from the GA optimisation provides insights into whether a parameter is positively or negatively correlated using the Pearson Correlation Coefficient. Figure 7 presents the most significant correlations for the GA optimisation in Sweden under the C1 constraints, while a comprehensive correlation analysis for all locations and constraints is available in the Appendix.

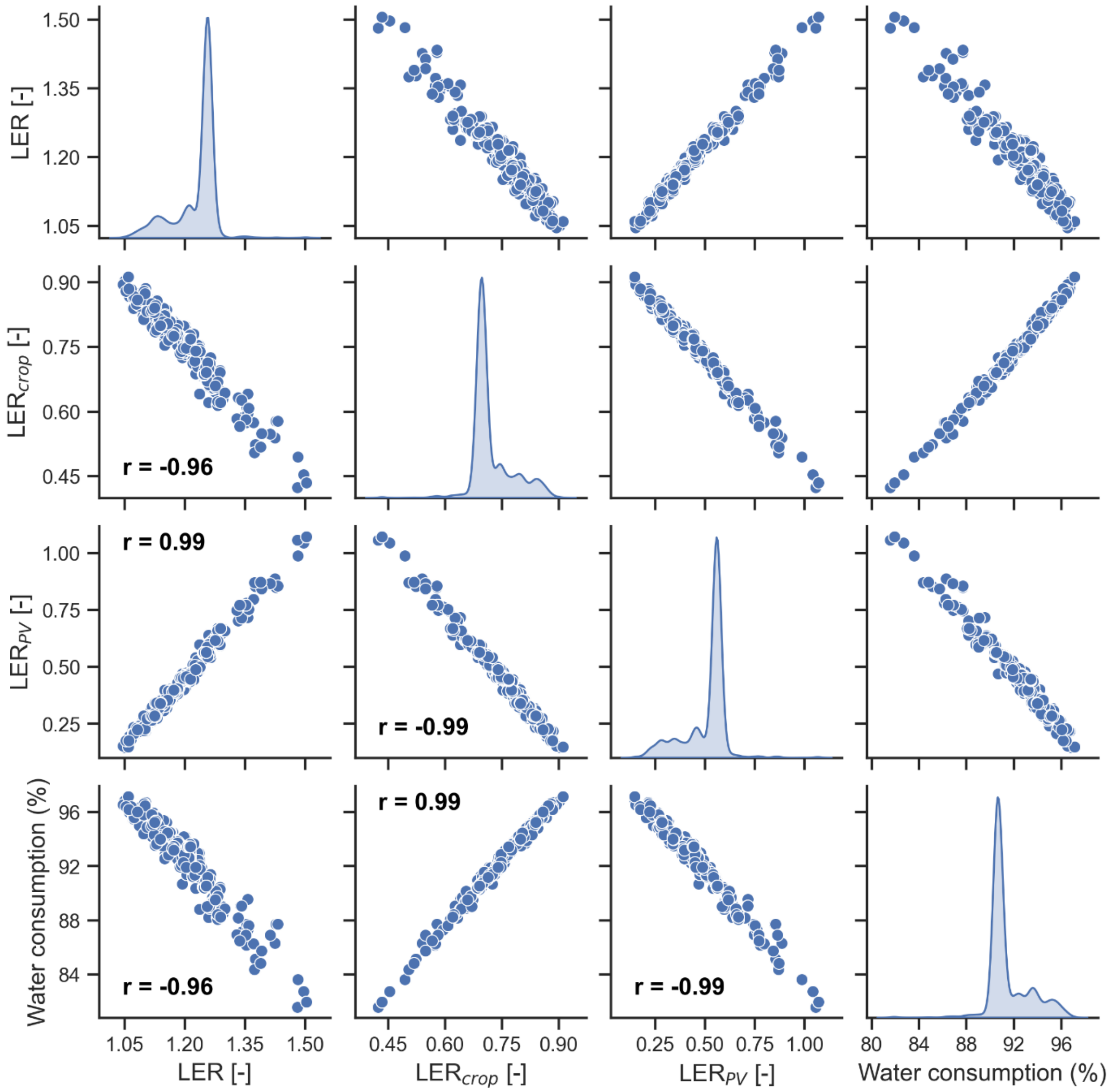

Figure 7. WEF-scenario key parameter correlations for Sweden when optimising under the C1 constraints.

The results clearly indicate a strong trade-off between crop yield and yearly electricity production, with a near-perfect negative correlation of −0.99. Additionally, LER_{crop} exhibits a strong negative correlation of −0.96 with LER, whereas LER_{PV} shows a high positive correlation of 0.99 with LER. This suggests that optimising LER without constraints would primarily favour LER_{PV}, as it has a greater overall impact than LER_{crop}. Furthermore, water consumption is strongly influenced by row pitch, showing a correlation of 0.85. Additionally, LER_{PV} exhibits a strong negative correlation with water consumption (−0.99), while LER_{crop} is highly positively correlated with it (0.99). This highlights the balance between increasing electricity production and managing water use in system design. In the Appendix, the correlation between each parameter, including row pitch, height, PV orientation, and system type for the WEF-scenario and location are presented. In C1 for Sweden the row pitch has a negative correlation of −0.85 with LER, a finding consistent with the optimisation results of Campana et al. [20] for vertical APV systems. This highlights that maximising LER would lead to minimising row pitch, but at the cost of a drastic reduction in crop yield, underscoring the need for policy constraints that regulate land use and crop yield. Interestingly, the correlation of PV orientation, height, and system type with LER, LER_{PV}, and LER_{crop} varied significantly across locations and scenarios, even though they were not the most influential parameters. The correlation between PV orientation and LER ranged from −0.20 to 0.17, depending on the optimisation convergence. In some cases, PV orientation had a greater impact, while in others, system type or height played a more dominant role. Conventionally, vertical systems are designed with east- or west-facing PV modules, one-axis trackers follow an east-west tracking strategy, and overhead systems are typically south-facing, yet these configurations may not always be optimal based on site-specific conditions and the given objectives.

3.2 Sensitivity analysis for agrivoltaic systems

To further investigate the optimal parameters in commonly used APV system configurations, it is essential to understand how each parameter influences each KPI, and the trade-offs considered by the GA algorithm. Figure 8 below presents a sensitivity analysis using a vertical system east-west oriented, with a 10 m row pitch and a height of 0.5 m as the baseline. This analysis examined the impact of row pitch, PV orientation, and height on LER, LER_{PV}, LER_{crop}, PAR reduction, and water consumption. Additionally, the optimal points for C1 and C2 are included to illustrate where the optimal solutions are located. The standard deviation for each year is also displayed to highlight year-to-year variability, which depends on the weather year and crop type within the crop rotation. Consistent with the findings from the GA correlation analysis, row pitch has the most significant influence on all KPIs. It is also evident that PAR reduction is greatest at higher latitudes, which in turn affects crop yield. Furthermore, smaller row pitches lead to greater year-to-year deviations, which is visualised in Figure 8 as a wider shaded area around the mean indicating increased overall uncertainty. A similar pattern is observed around 0° PV orientation, where there is a slight increase in LER_{crop}, a trend that was leveraged in the GA optimisation to satisfy the C2 constraints in Italy. Water consumption also plays a more significant role in Italy compared to Sweden, as the drier climate and higher ET rates make water availability a more critical constraint. This results in greater sensitivity to row pitch and PV orientation in Italy, as shading strategies must balance both crop yield and water use efficiency. In contrast, in Sweden, where precipitation levels are higher and water scarcity is less of a concern, the optimisation focuses more on trade-offs between PV production and crop yield, with water consumption playing a less decisive role. In some cases, the optimal points fall below the KPI values in the sensitivity analysis, as those sensitivity values would not satisfy the crop yield constraints, as seen in the LER vs row pitch results for Germany. Conversely, in cases like LER vs PV orientation in Germany, crop yield was deliberately reduced to increase PV yield using a different system type, ultimately improving LER. A sensitivity analysis for one-axis and overhead systems is provided in the Appendix.

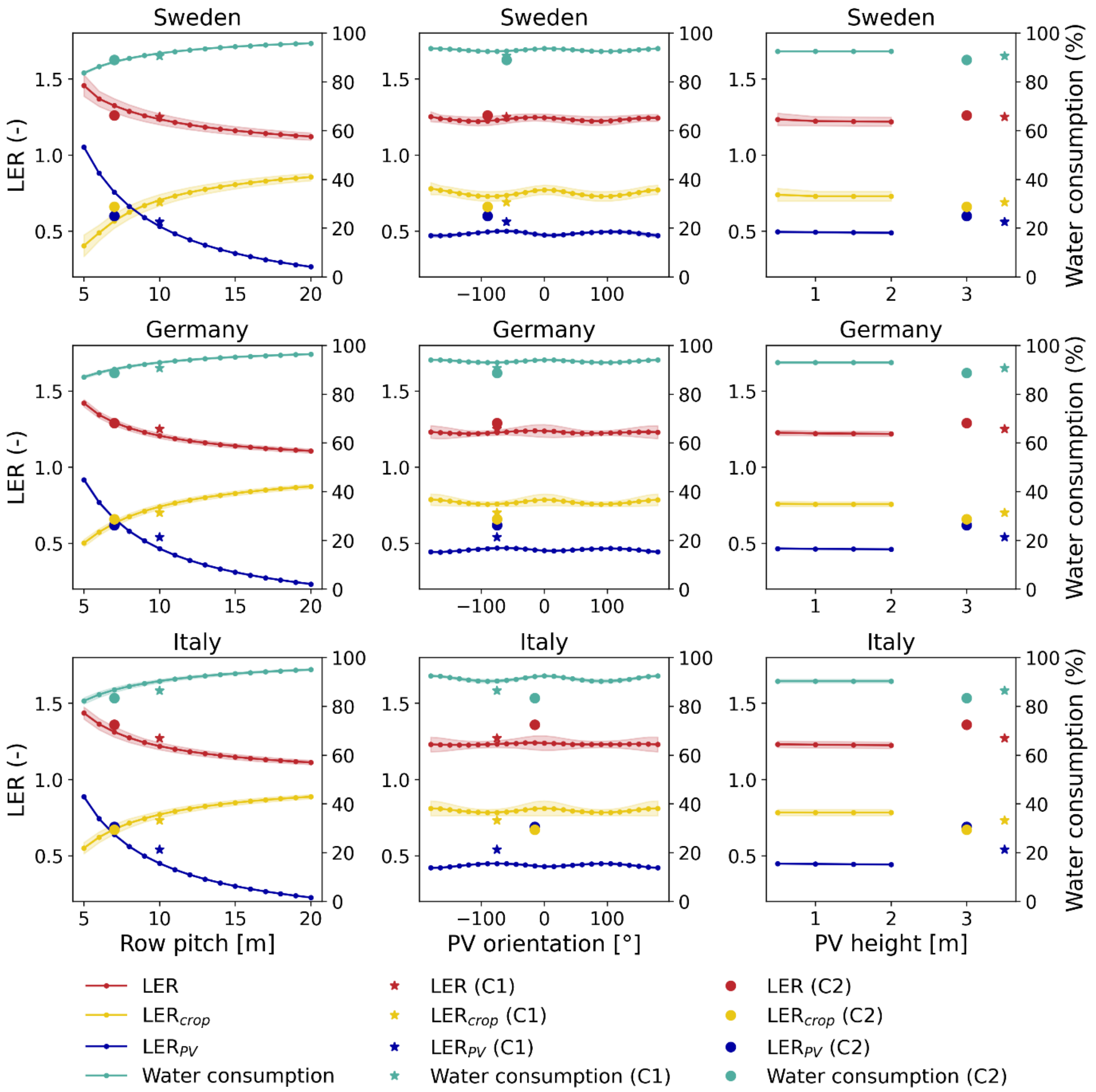

Figure 8. Sensitivity analysis of row pitch, PV orientation, and height on system KPIs. Results are based on a vertical east-facing system (10 m pitch, 0.5 m height). Results correspond to the WEF scenario. Stars indicate optimal solutions identified by the GA under the C1 constraint, while circles represent optimal solutions found under the C2 constraint.

To explore how row pitch affects land-use efficiency in different settings, we compared LER, LER_{crop}, LER_{PV} across vertical, one-axis, and overhead systems in Sweden, Germany, and Italy (see Appendix). Overall, LER decreases with increased row pitch in all locations, confirming that closer spacing improves total land-use efficiency. LER_{crop}, however, increases with row pitch due to better light availability for crops, particularly in vertical systems and in Italy, where high irradiation enhances crop performance. In contrast, LER_{PV} decreases with wider spacing, as expected, due to reduced panel density. These trends and geographical differences are detailed further in the Appendix.

The year-to-year variation in LER was particularly pronounced at smaller row pitches, where increased shading made the APV system more dependent on weather conditions with high irradiance to maintain optimal crop yields. However, this variability is not solely attributable to row pitch. The choice of crop for a specific weather year also plays a significant role. In this study, we applied a consistent crop rotation scheme across all weather years. Nevertheless, an optimisation algorithm might yield entirely different results if the crop-year allocation were allowed to vary. In Figure 9, interannual differences in performance are evaluated using a one-axis east–west tracking APV system with a 2 m axis height and spring wheat as the reference crop, for the years 2018 and 2023. These years were chosen as they represent the highest variation in performance, with 2018 and 2023 showing the lowest and highest precipitation levels for Sweden and Germany, respectively, while maintaining relatively balanced conditions for Italy. This selection allows for a clear comparison of performance differences under varying climatic conditions.

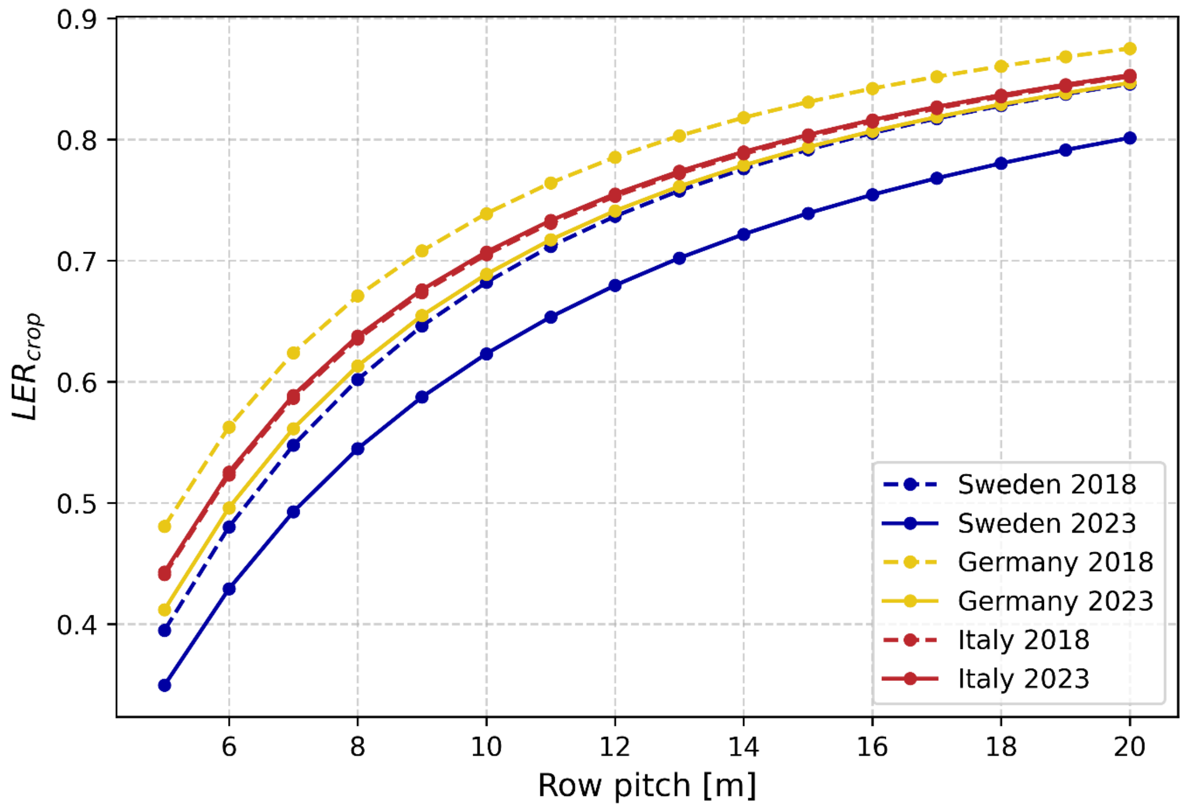

Figure 9. Simulated LERcrop of a one-axis east–west tracking APV system (2m axis height) with spring wheat in 2018 and 2023 for three locations: Italy, Germany, and Sweden.

Notably, in Italy, the LER_{crop} for spring wheat remained relatively stable between these two years. In contrast, Sweden and Germany exhibited substantial differences. Interestingly, these variations were not limited to small row pitches, significant deviations were also observed at larger row pitches, highlighting that weather conditions, rather than row pitch alone, are the dominant factor driving year-to-year variability in LER_{crop}.

4 Discussion

4.1 Limitations

In this study, we introduce an optimisation framework that enables the weighting of different objectives, such as crop yield retention, electricity production, and water conservation, to explore optimal APV configurations under varying policy scenarios and site-specific conditions. However, it is important to note that we did not attempt to identify an "optimal" set of weights, nor do we claim to establish a universally valid trade-off hierarchy. The selection of weights remains a user-defined input, reflecting the priorities of stakeholders or regulatory schemes, and falls outside the scope of this study. While this approach offers flexibility, it also introduces subjectivity. In contrast, recent studies have implemented structured weighting schemes, such as the ordinal priority approach (OPA) combined with technique of order preference similarity to the ideal solution (TOPSIS), to derive weights based on expert elicitation and stakeholder ranking [38]. Such methods can formalise and balance input from diverse groups (e.g., agricultural researchers, energy specialists, farmers, and developers) by translating qualitative preferences into quantitative weights. Future research could build on our framework by integrating participatory or data-driven approaches for weight determination. Techniques such as OPA, analytic hierarchy process (AHP), or machine learning-based preference inference could be explored to better capture stakeholder priorities in real-world decision-making contexts. This would enhance the practical relevance and legitimacy of multi-objective optimisation results in APV planning.

One important limitation in our current analysis is the lack of consideration for increased CAPEX associated with changes in system height. In

Table 5, no height-dependent costs are included, even though taller APV structures typically require more robust foundations and support structures, which would raise installation costs. Since CAPEX is calculated per kWp, systems with the same installed capacity but different heights could have significantly different total costs, something not currently captured in the model. Additionally, while operation and maintenance costs are set at 1% of CAPEX annually, this may underestimate the true cost for one-axis tracking systems, which involve additional mechanical components and complexity. Lastly, we rely on a fixed set of economic input parameters (e.g., CAPEX, electricity price, crop profit), but these values can vary widely across regions, policy environments, and over time. This is also shown by Zidane et al. [50].

Another key limitation lies in the crop modelling. The EPIC model simulates crop yield as a function of intercepted PAR, which is itself governed by LAI and its development over time. In our simulations, LAI parameters are fixed per crop and do not dynamically respond to changes in light availability. However, experimental studies have shown that many crops can physiologically adapt to partial shading, for instance by increasing leaf area or altering canopy structure, thereby improving light interception and mitigating yield losses [28,59]. Since EPIC does not account for such phenotypic plasticity, our simulated yields under shading can be interpreted as worst-case estimates, and the actual LER achieved in practice may be higher than those predicted. In the results presented, particularly with the Italian constraints (C3), it may be necessary to use crop models calibrated for shading conditions or with a high mechanistic level capable of simulating adaptation mechanisms under shading. This was evident, as increasing the maximum LAI and RUE allowed the system to meet both Italian regulations and best practices simultaneously. Additionally, further improvements to the crop model could involve the development of LAI datasets that would help better estimate crop yield based on measured data. Moreover, albedo was assumed to be 0.2 in the simulations, but considering that albedo can vary between different crops [60], assuming a higher albedo could potentially increase PV production. This, in turn, could make the Italian scenario S3 more likely to be feasible without increasing maximum LAI and RUE.

Another limitation of this study lies in the assumption of a fixed tilt angle of 35° for all overhead APV systems and for the conventional ground-mounted PV reference system. While 35° is a commonly used tilt angle in European PV design and provides a reasonable approximation across different latitudes, it may not represent the optimal configuration for each specific location. Optimal tilt varies with latitude and seasonal solar trajectories, and site-specific optimisation could yield marginal gains. Nonetheless, prior studies have shown that tilt angles in the range of 30−40° generally perform close to optimal across a broad range of latitudes throughout Europe [61,62].

Lastly, one important limitation concerns the formulation of the crop component (LER_{crop}), as expressed in Equation (1). In our study, we apply a reduction factor (χ) representing the fraction of land considered harvestable under APV conditions, and multiply this with the simulated crop yield under the APV system. This accounts for zones near PV rows that are assumed to be obstructed or otherwise not suitable for cultivation. However, this approach introduces two related sources of uncertainty. First, the spatial averaging of irradiance used in our crop simulations includes the full row spacing, both harvestable and non-harvestable areas. This means that the simulated yield reflects the average light availability across the entire APV row pitch, even though some edge zones are not actually cultivated. A more precise approach might involve excluding these non-harvestable-zones from the irradiance averaging when estimating crop growth, so that the simulated yield better represents conditions only in the actively cultivated areas. This adjustment would likely affect the estimated yield under APV conditions and, consequently, the resulting LER_{crop} values. Second, the way the reduction factor is applied may introduce a systemic bias in favour of APV systems. The common formulation is that the reduction is applied to the APV yield, not the open-field reference. As a result, when the APV yield is lower than the open-field yield, the land loss appears smaller in relative terms, leading to optimistically high LER_{crop} values. Conversely, if the APV system results in a higher yield than the open-field reference (e.g., due to improved microclimate), the current approach overestimate the reduced yield based on the area that is not cultivated. This asymmetry could distort comparative assessments of land-use efficiency across different system designs or environmental conditions. To address this, future studies might consider an alternative formulation that subtracts the yield potential of the non-harvestable fraction based on the open-field reference:

$$LER_{crop} = \frac{Y_{c,APV} - \left[(1-\chi)Y_{c,ref}\right]}{Y_{c,ref}}, \tag{10}$$

This expression better reflects the opportunity cost of excluded land by referencing it to the baseline open-field productivity, offering a more conservative and balanced estimation of LER_{crop}.

4.2 Policy constraints in APV systems

Our findings reveal that the viability of APV systems is highly sensitive to the structure of national and regional policy frameworks. C3, which combines national policy regulation with recommended best practices, did not produce any feasible solutions across the tested locations. This outcome illustrates how strict and overlapping constraints can limit the range of viable system configurations. In C3, requirements included a minimum PV output of 60%, a maximum land occupation of 30%, a crop yield reduction of 30%, and a height restriction on the structure. While each of these individually aims to support a balance between food, energy, and landscape protection, their combined application resulted in a design space so narrow that no solution met all criteria. In this study, we modelled crop yield reductions as directly influencing the PLV, assuming a one-to-one relationship where a 1% yield loss corresponds to a 1% reduction in PLV. Although this does not reflect an explicit policy constraint, it allowed us to estimate how reduced productivity might affect the perceived value of the land under incentive schemes such as the Italian national recovery and resilience plan (PNRR) [44]. However, this modelling assumption is a simplification and reflects a limitation in the simulation framework. In reality, PLV is influenced by more than yield. For example, certain high-value crops such as wine grapes may retain or even increase their market value when produced under APV, due to sustainability branding or added marketing potential [63]. This highlights the importance of interpreting policy thresholds like yield loss or land value in a flexible and context-aware manner. If we had removed the crop yield constraint from C3 while keeping the other constraints, would actually have been less strict than the Swedish (C1) and German (C2) constraints. In such case, our optimisation suggests that the system would converge toward configurations with very narrow row spacing. This would maximise energy yield but result in significant reductions in crop productivity. While technically optimal from an energy standpoint, such outcomes are clearly undesirable in terms of agricultural performance and long-term food security.

It is also worth reflecting on the interaction between the crop yield constraint and the land occupation threshold. Both are intended to safeguard agricultural function, but applying them simultaneously may not always be necessary. In fact, one potential improvement to the design of S3 could involve removing the explicit yield constraint while instead applying a stricter limit on maximum land occupation. This would simplify the regulatory framework while still indirectly protecting crop productivity. We also observed that small changes to input parameters related to crop behaviour under shading were enough to shift the scenario from completely infeasible to feasible. This reveals a critical challenge. Policies that rely on narrow thresholds leave little room for uncertainty and place heavy demands on simulation accuracy and data quality. For developers and practitioners, this increases the complexity and risk of project planning, particularly when site-specific responses are difficult to predict.

Altogether, these findings suggest a need for greater transparency and adaptability in the way policy constraints are defined and applied. Thresholds should be based on robust evidence and allow for site-specific flexibility, considering crop type, regional solar potential, and market context. Rather than enforcing rigid criteria across all regions, regulatory frameworks could benefit from guidance that helps developers interpret requirements in ways that remain faithful to policy goals while enabling practical implementation. The role of policy intermediaries and brokers becomes central in this process, helping to translate complex regulations into workable design strategies that reflect the realities of both farming and energy conversion [64].

4.3 Interannual variability and system robustness

Interestingly, despite using multi-year weather data and a six-year crop rotation, our results showed relatively limited interannual variation in KPIs across the evaluated sites. This stability appears to result from a combination of factors, potentially including the selection of crops that are generally considered more resilient to shading [34,35,65], although shade tolerance was not explicitly modelled in this study, site-specific climatic conditions, system configurations that moderate the effects of annual variability in solar irradiance, and the use of fixed crop model parameters that do not account for interannual phenotypic plasticity or year-specific crop responses. For instance, as shown in Figure 9, LER_{crop} values for spring wheat varied more noticeable between 2018 and 2023 in Sweden and Germany, which experienced higher interannual variation in precipitation, while the Italian site remained comparatively stable. These findings suggest that crop type, local climate, and panel layout jointly influence the year-to-year robustness of system performance. However, our sensitivity analysis shows that design parameters such as row pitch and PV orientation can amplify or dampen this variability. Narrower row spacing tends to increase shading, which in turn raises the standard deviation of KPIs like LER_{crop} and LER. Similarly, certain orientations introduce more variable irradiance patterns under the panels, making system performance more sensitive to yearly fluctuations. These results highlight that while the crops used in this study performed robustly under the tested conditions, this outcome may not generalise to crop types that are more sensitive to shading or to scenarios with more extreme climate stressors. Future research that includes a broader range of crop sensitivities and weather scenarios could reveal stronger interannual trade-offs and offer additional insight into the resilience and adaptability of APV designs under real-world conditions.

4.4 Trade-offs: economics and WEF prioritisation

Another major insight from our optimisation results is the inherent trade-off between food and energy conversion, consistent with broader sustainability system integration principles [66]. The GA correlation analysis showed a nearly perfect inverse relationship between crop yield and PV output (Pearson $r \approx -0.99$), confirming that increased panel density or lower row spacing, favourable for electricity production, generally reduces PAR available to crops. These trade-offs varied across locations: warmer and sunnier locations like Piacenza in Italy allowed higher total LER, benefiting from favourable conditions for both crop growth and PV output.

Importantly, our results show that optimal system design is sensitive to the weights chosen. For instance, removing water from the WEF nexus in the EF scenario led to distinct shifts in system type and PV orientation. More notably, when economic performance was explicitly included, as in the WEEF scenario, designs shifted toward configurations that prioritised long-term financial viability. This often involved modifying row pitch and system type to increase revenue from electricity while still satisfying crop yield constraints, demonstrating that the inclusion of economic objectives fundamentally alters the optimisation landscape. While our analysis used low-input rotational cropping systems to ensure comparability, these may not reflect economically optimal farming practices [50,67]. In real-world settings, high-value crops such as tomatoes [68], could shift the objective from maximising biophysical efficiency (e.g., LER or water use) toward maximising income.

5 Conclusion

This study presents a multi-objective optimisation framework for evaluating APV systems across three European locations with varying climate conditions and regulatory constraints. The optimisation integrates water, energy, and food objectives using a normalised weighted-sum method, which converts multiple objectives into a single linear performance index. This allows for systematic exploration of trade-offs and priorities under different stakeholder perspectives and policy scenarios. The key findings are:

- Row pitch was consistently the most influential parameter in system design. Optimal spacing typically ranged between 5–10 m across locations and scenarios, strongly affecting both light availability and land-use efficiency.
- A strong trade-off was confirmed between PV output and crop yield, with a correlation of −0.99, indicating that optimisation must carefully balance electricity generation with food production goals. Water consumption was positively correlated with crop yield (0.99) and negatively correlated with PV output (−0.99), meaning that designs optimised for energy reduce water use due to increased shading and lower ET, but at the cost of reduced crop productivity.
- A strong linear relationship was found between the yearly average AOI, defined as the angle between the PV module surface and incoming sunlight, and the yearly average

PAR reduction on the ground. Lower average AOI values, resulting from orientation strategies that intercept more direct sunlight, increased PV output but led to larger reductions in under-panel PAR. This finding illustrates a key design trade-off in APV systems, where maximising electricity production can reduce the light available to crops.

- Differences between scenarios were shaped more by the type of constraint than by its strictness. The Swedish constraints (C1) applied a strict land occupation limit but did not constrain crop yield directly. This led to wider row spacing and resulted in equal or higher crop yields compared to the German constraints (C2), which had a more lenient land occupation threshold but imposed an explicit yield loss constraint. This illustrates how policy design choices influence system outcomes and should be carefully aligned with overall APV goals.
- The combined Italian guidelines and best practices constraints (C3) applied several strict constraints, including minimum PV output, maximum land occupation, allowable yield loss, and a system height limit. This led to no feasible solutions across sites. However, scenario feasibility was highly sensitive to crop model inputs such as RUE and maximum LAI. Small changes in these key parameters made the scenario feasible, indicating that rigid regulatory thresholds may over constrain design unless supported by highly accurate APV integrated modelling platforms, which is often difficult to achieve in practice.
- Simulations showed relatively low interannual variation in performance across years, crops, and locations. This stability can be attributed to several factors: the inclusion of shade-tolerant crops such as ley grass in the rotation, the use of a balanced multi-year crop rotation, and system configurations that moderate the effects of annual solar variability. However, this observed stability may also reflect the use of fixed and uncalibrated crop model parameters, which do not account for interannual variation in crop responses or phenotypic plasticity. Sensitivity analysis further revealed that system variability increases with decreasing row pitch and with less conventional PV orientations, suggesting that bot design configuration and crop-specific weather interactions influence performance robustness. These findings also highlight a broader challenge: robust calibration of crop parameters is difficult, especially under APV conditions, as it would ideally require multi-year, multi-environment datasets that capture both open-field and shaded growth dynamics.

Acknowledgements

The authors acknowledge the following funding agencies and related projects: the Swedish Energy Agency for the projects SOLVE (grant number 52693-1) and "Evaluation of the first agrivoltaic system facility in Sweden to compare commercially available agrivoltaic technologies (MATRIX)" (grant number P2022-00809). Additionally, the author Pietro Elia Campana would like to acknowledge Formas - the Swedish Research Council for Sustainable Development - for the funding received through the early career project "Avoiding conflicts between the sustainable development goals through agro-photovoltaic systems" (grant number FR-2021/0005). The authors also thank Alessandra Scognamiglio and Celeste Mellone for their valuable assistance with policy-related guidance and support throughout this work.

Appendix

This Appendix provides extended analyses and supplementary results that support the main findings of this study. It includes sensitivity analyses, correlation assessments, comparative system evaluations, and a model validation, all conducted to strengthen the robustness and generalisability of the study outcomes. To complement the sensitivity analysis of the vertical APV system, additional assessments were performed for one-axis (Figure A1) and overhead (Figure A2) configurations. The analyses evaluated the influence of row pitch, PV orientation, and module height on the following KPIs: LER, LER_{crop}, LER_{PV}, and water consumption. The results confirm that row pitch consistently exerts the strongest influence on system performance across all configurations and climates. PV orientation has a moderate effect, especially in warmer regions, while module height was found to have a comparatively limited impact. As with the vertical system, narrow row spacing increased the interannual variability of KPIs, underscoring the trade-off between energy conversion and system resilience to weather fluctuations. Optimal configurations under C1 and C2 constraints are highlighted in each figure.

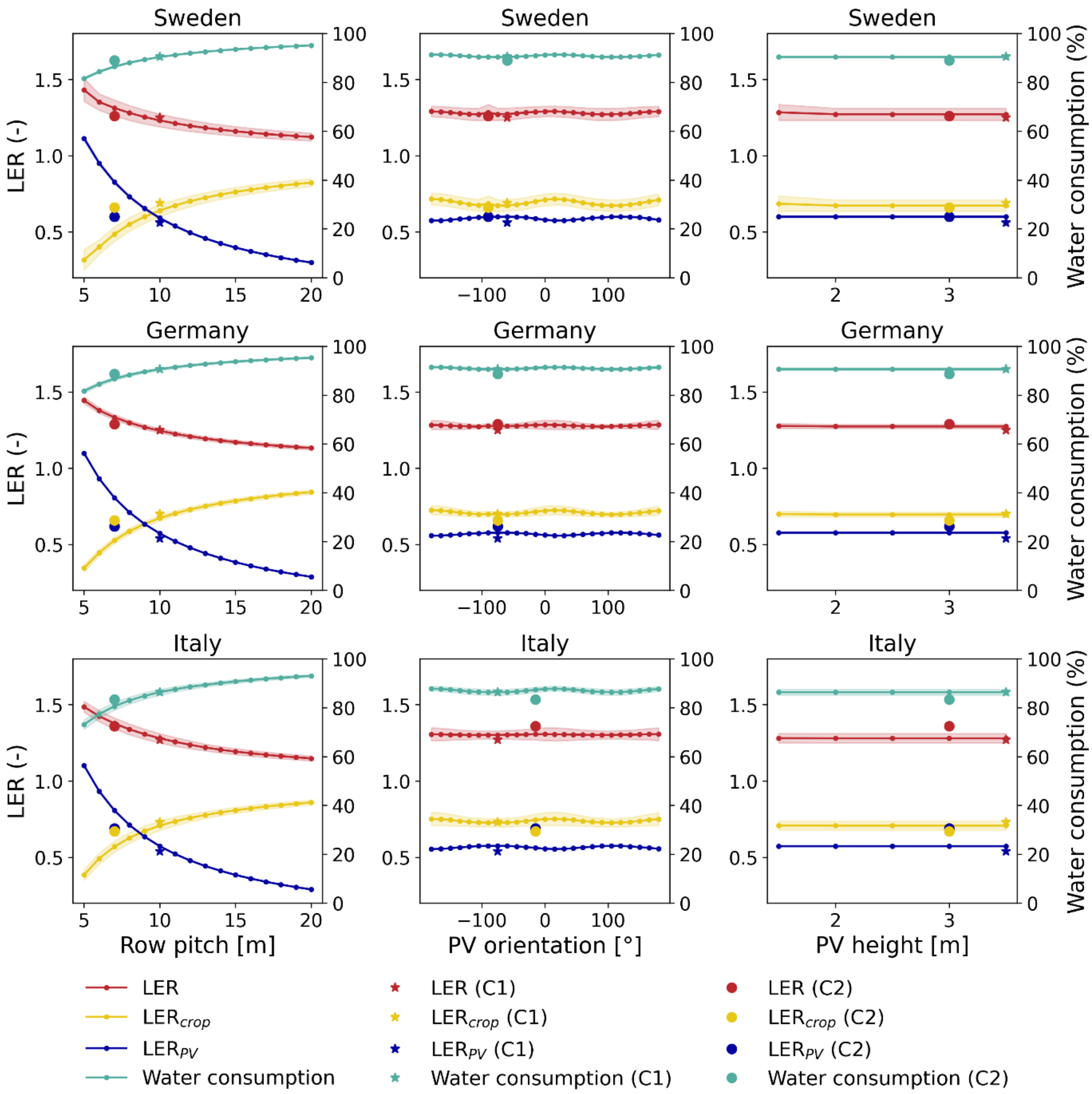

Figure A1. Sensitivity analysis of row pitch, PV orientation, and height on system KPIs. Results are based on a one-axis east-facing system (10 m pitch, 2 m height). Results correspond to the WEF scenario. Stars indicate optimal solutions identified by the GA under the C1 constraint, while circles represent optimal solutions found under the C2 constraint.

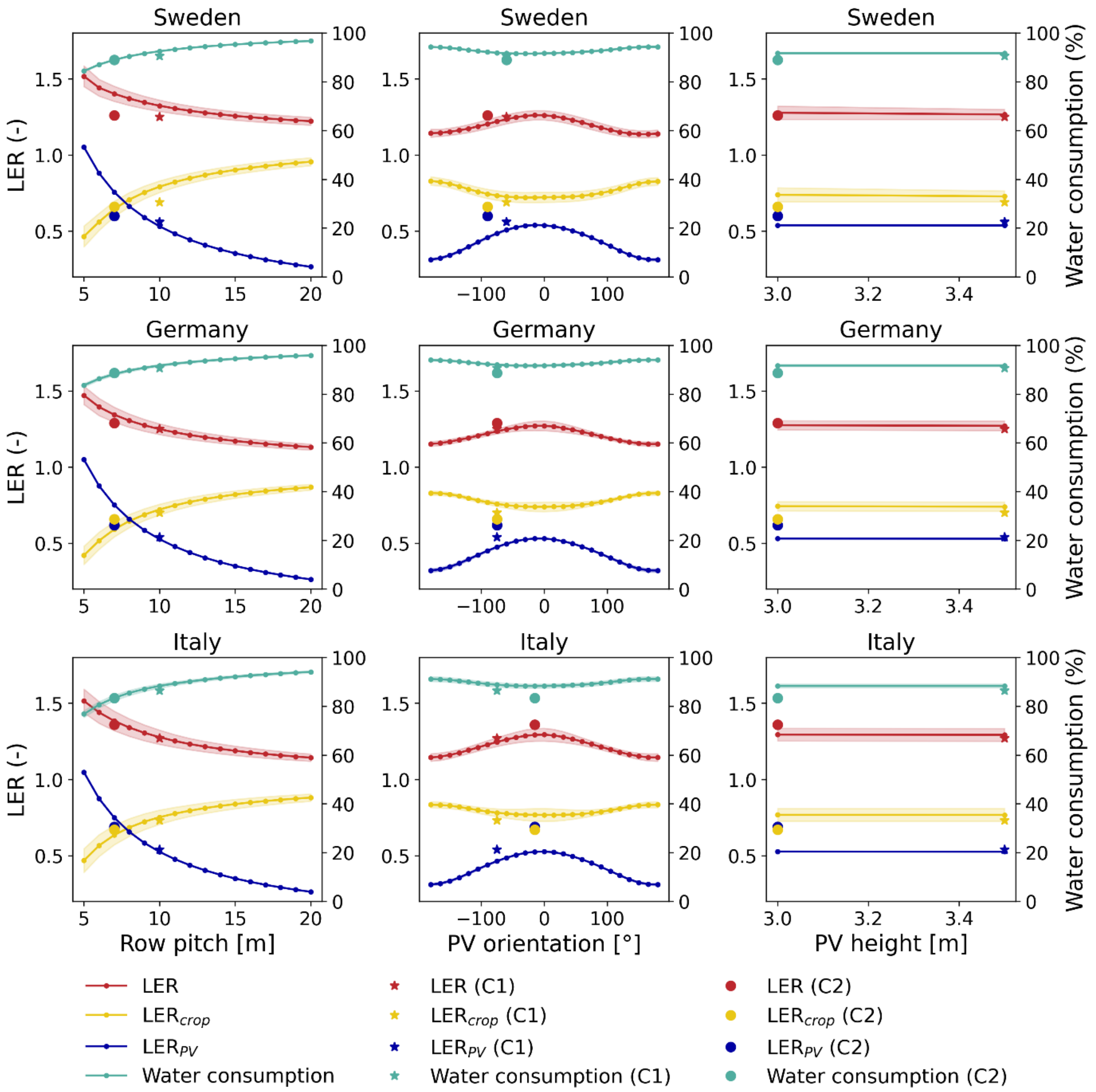

Figure A2. Sensitivity analysis of row pitch, PV orientation, and height on system KPIs. Results are based on an overhead south facing system (10 m pitch, 3 m height). Results correspond to the WEF scenario. Stars indicate optimal solutions identified by the GA under the C1 constraint, while circles represent optimal solutions found under the C2 constraint.

To better understand how each design parameter correlates with the system's performance outcomes, Pearson Correlation Coefficient were calculated. Figures (Figure A3-Figure A8) summarise the parameter correlations across all locations (Sweden, Germany, Italy) and policy constraints (C1 and C2). A consistent and strong inverse relationship between PV output and crop yield was found in every case, reaffirming the central design trade-off of APV systems. Row pitch emerged as the most influential parameter, with consistently high correlations to all KPIs. PV orientation, module height, and system type exhibited more location- and constraint-specific impacts. For stricter constraints (e.g., C2), system adaptation such as overhead structures and non-standard orientations were required to maintain yield thresholds.

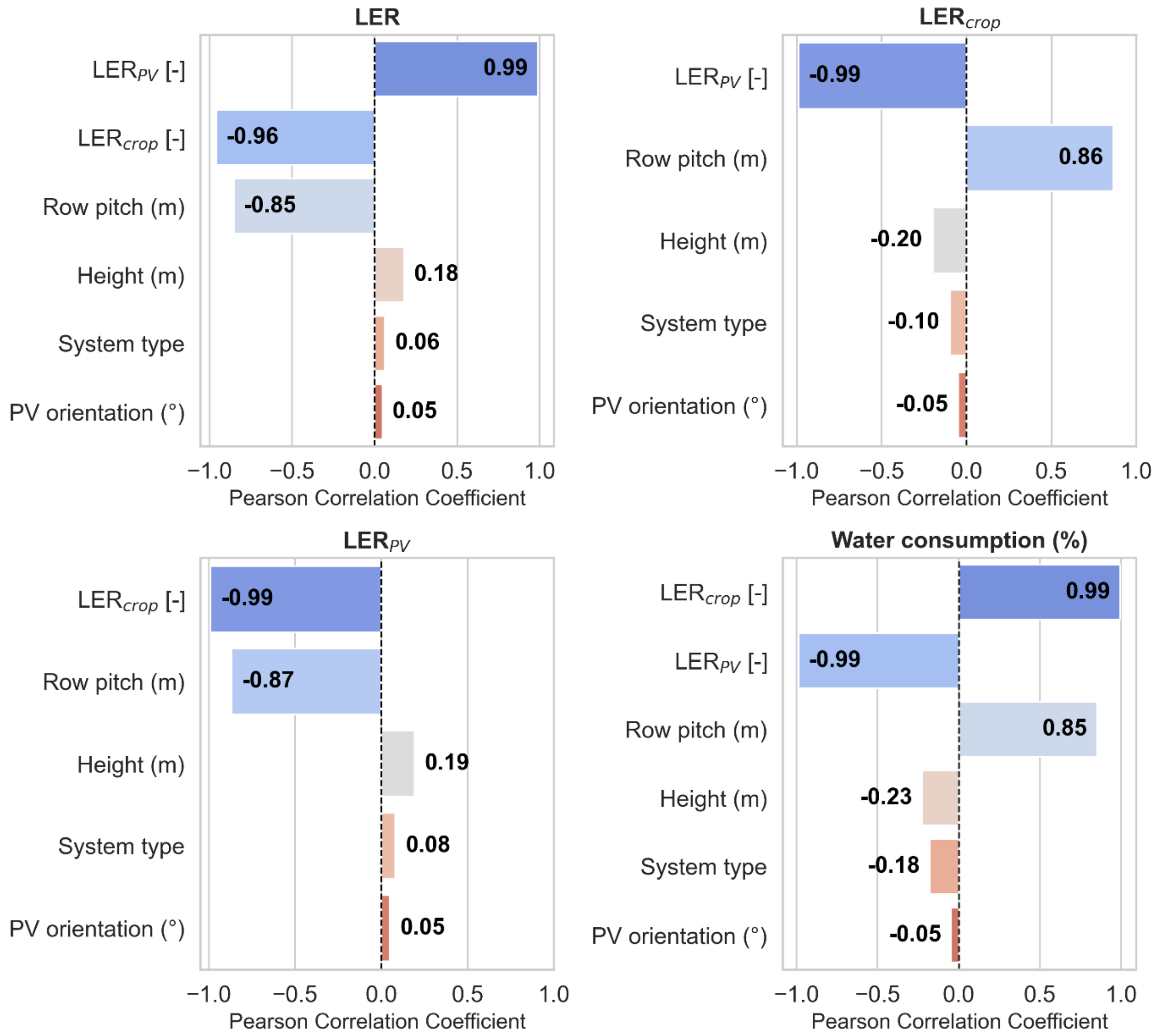

Figure A3. Correlation between each parameter for Sweden optimising for C1. Results correspond to the WEF scenario.

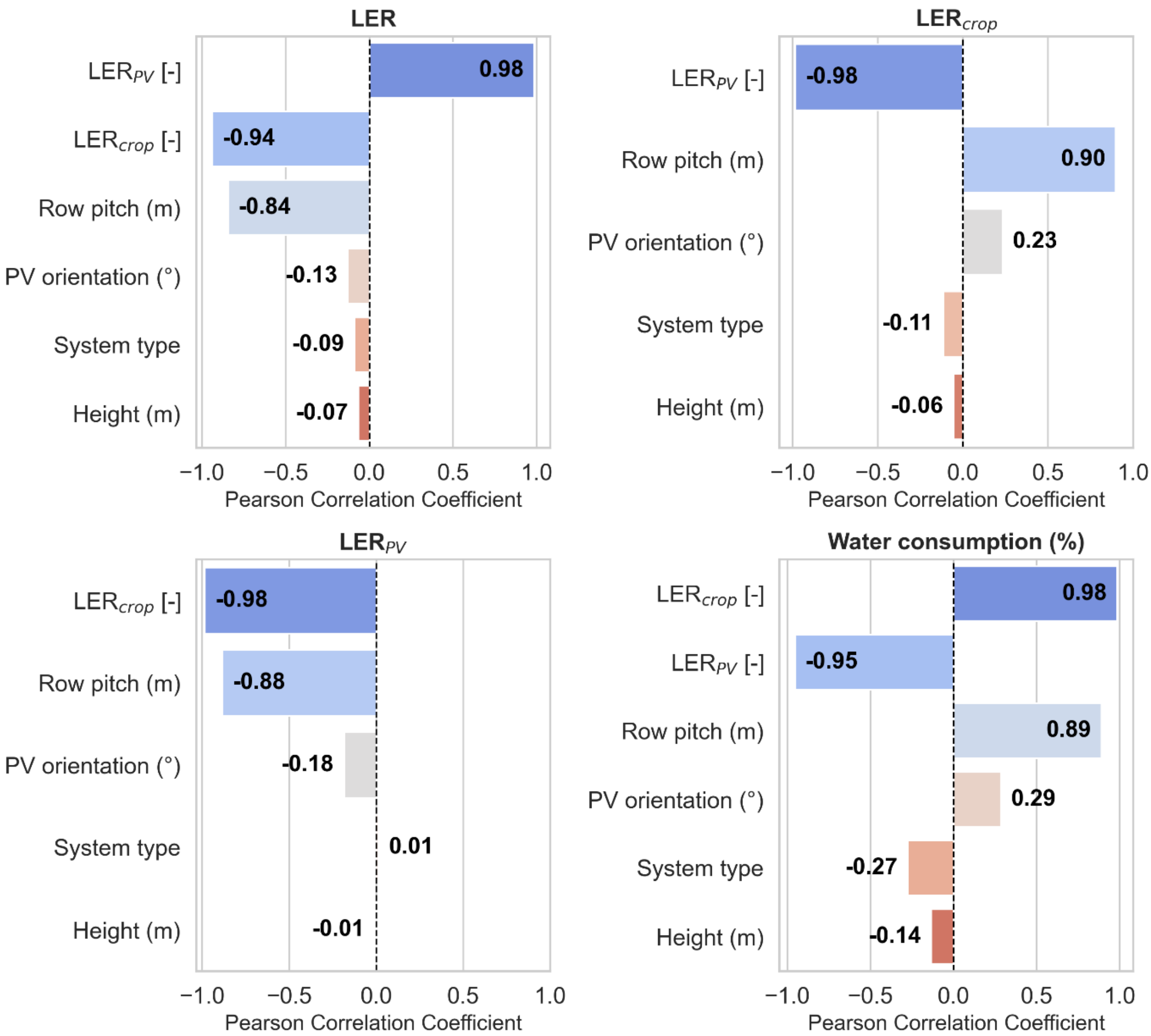

Figure A4. Correlation between each parameter for Sweden optimising for C2. Results correspond to the WEF scenario.

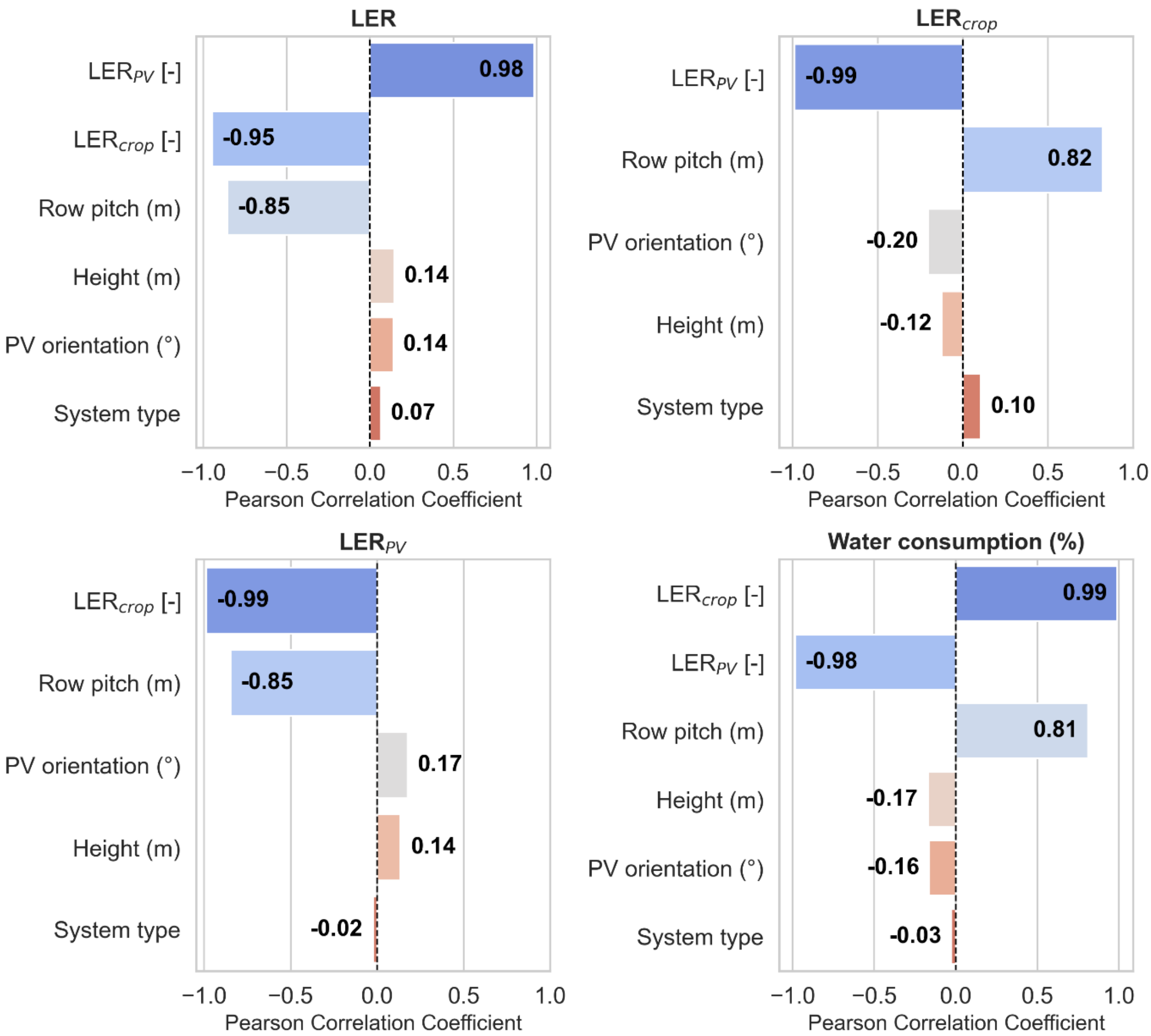

Figure A5. Correlation between each parameter for Germany optimising for C1. Results correspond to the WEF scenario.

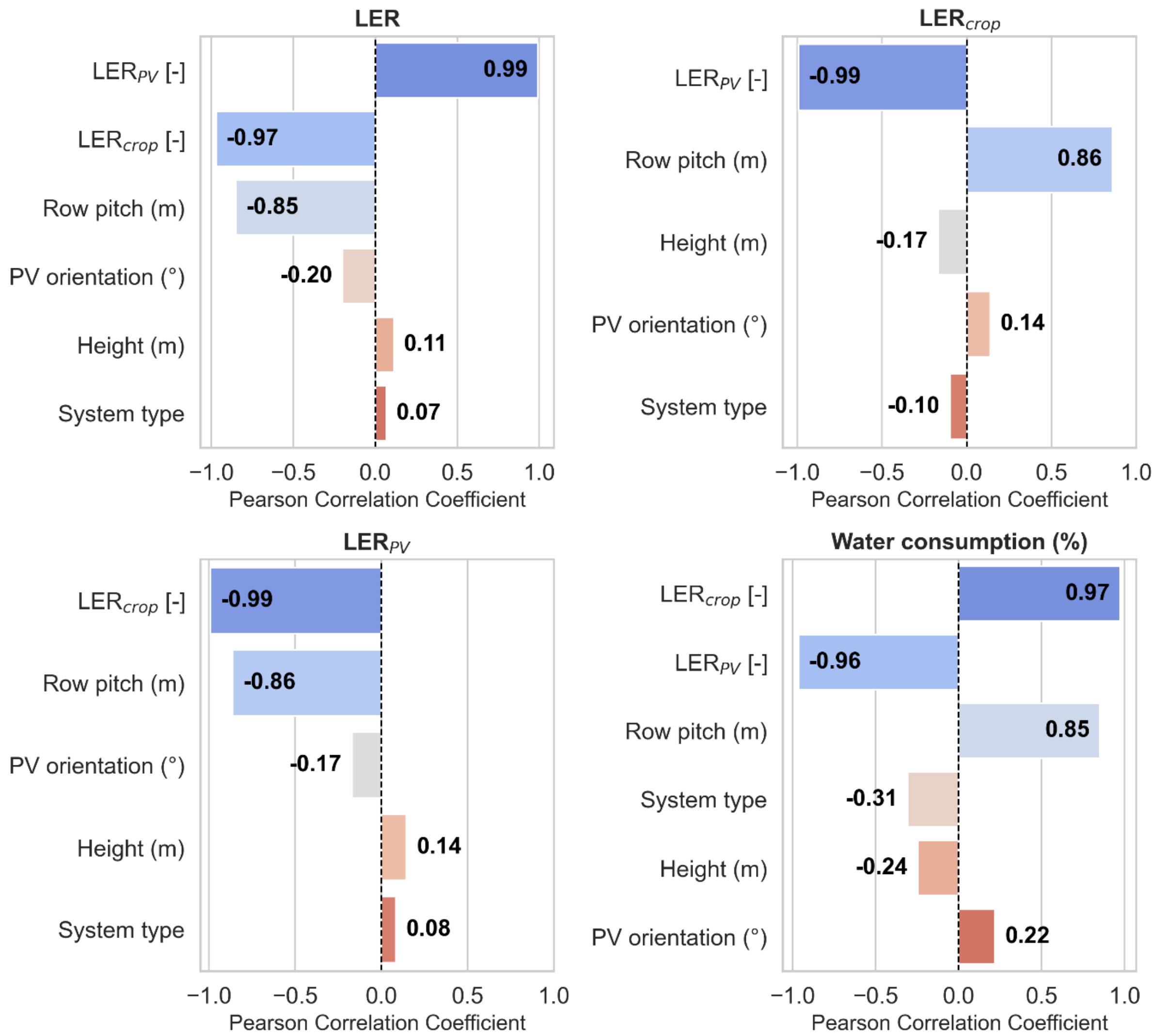

Figure A6. Correlation between each parameter for Germany optimising for C2. Results correspond to the WEF scenario.

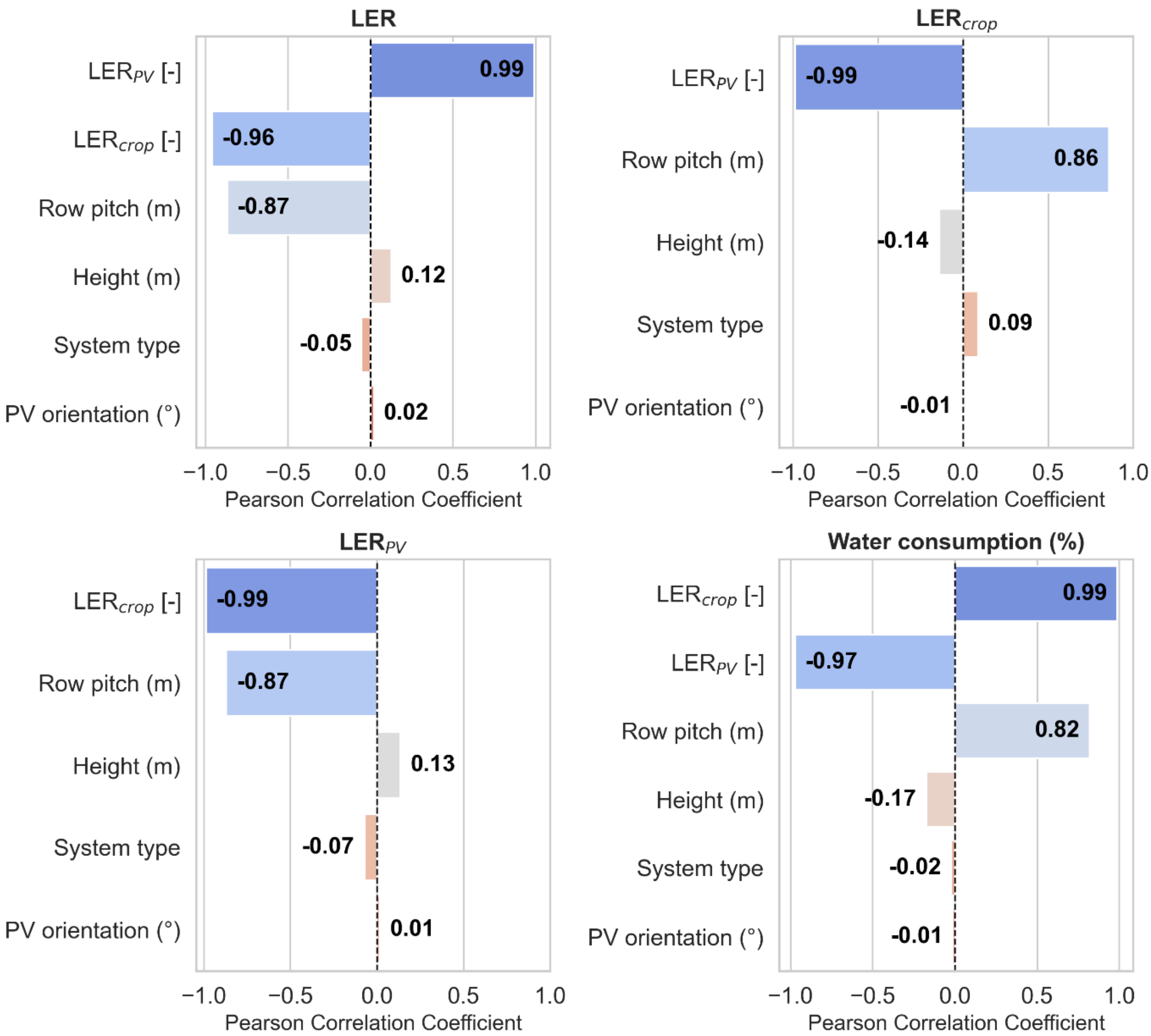

Figure A7. Correlation between each parameter for Italy optimising for C1. Results correspond to the WEF scenario.

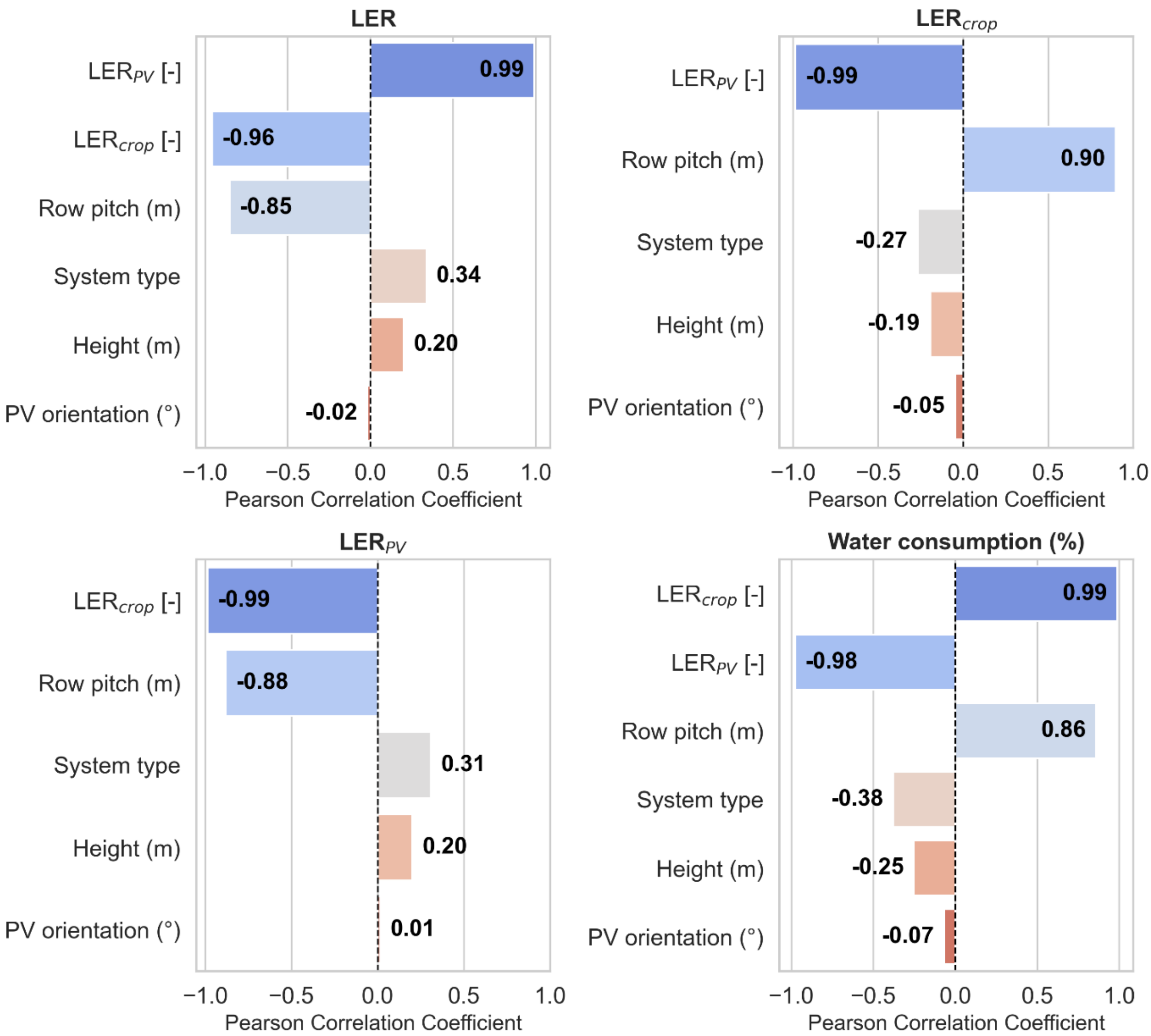

Figure A8. Correlation between each parameter for Italy optimising for C2. Results correspond to the WEF scenario.

To compare the performance of different APV configurations, simulations were conducted for vertical, one-axis, and overhead systems across a range of row pitches in Sweden, Germany, and Italy (see Figures Figure A9-Figure A11). Notably, vertical systems tend to yield the highest LER$_{crop}$. Conversely, one-axis tracking systems often achieve the highest LER$_{PV}$ due to sun-tracking capability. This comparison illustrates that system selection should be based on site-specific priorities, balancing energy conversion with crop protection and regulatory thresholds.

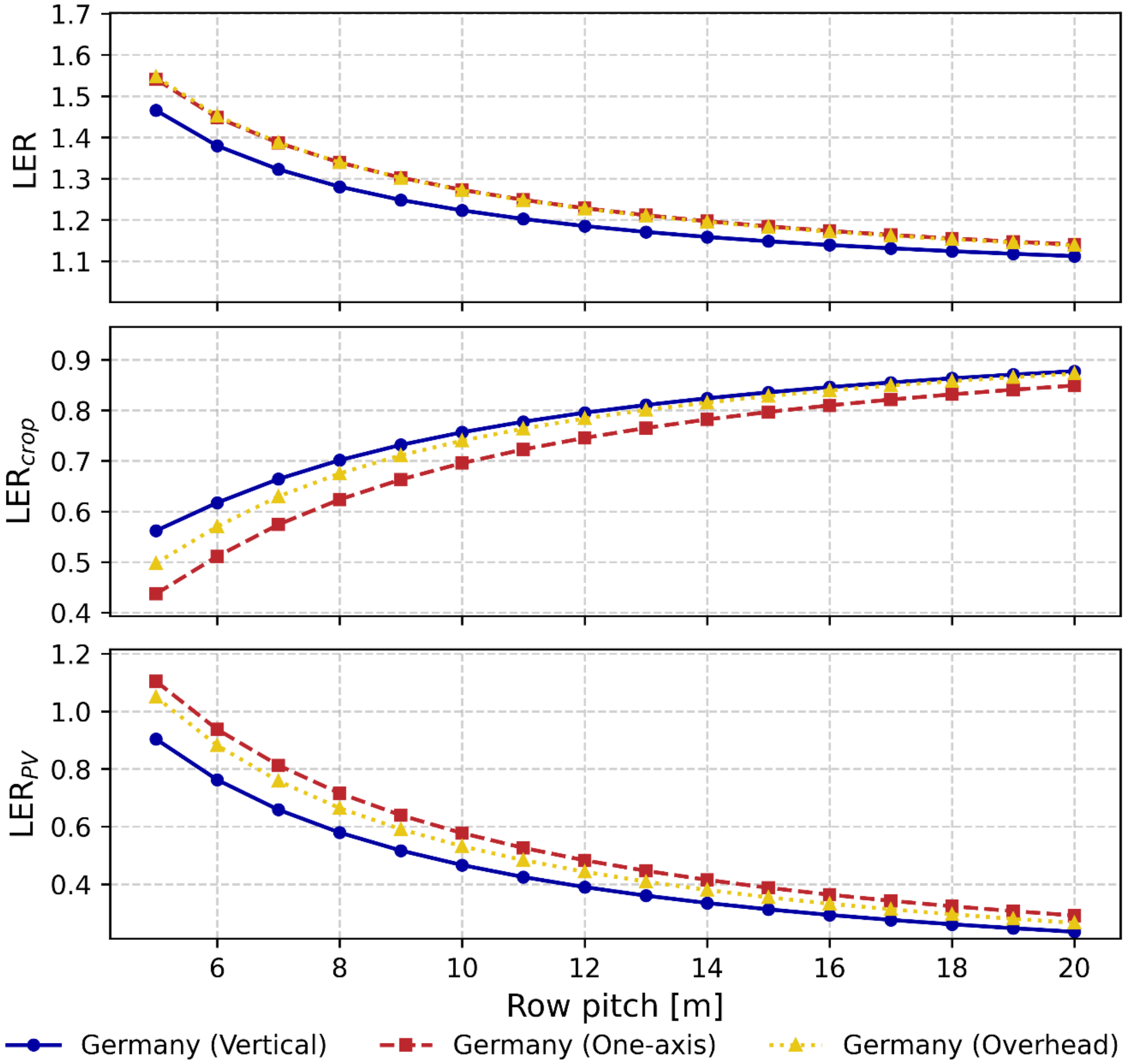

Figure A9. Comparison of LER, LER_{crop}, and LER_{PV} in Germany for different APV system designs as a function of row pitch.

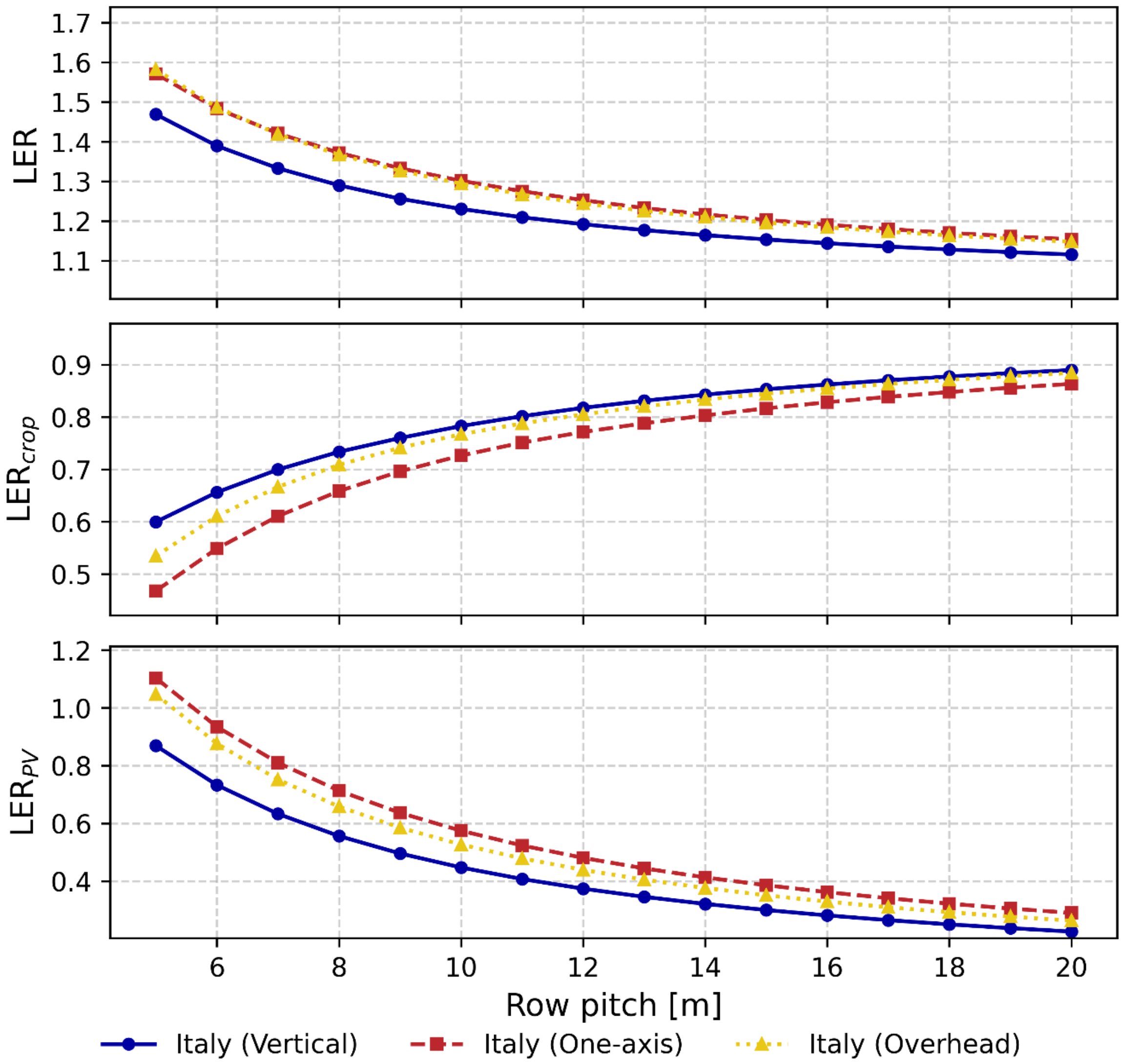

Figure A10. Comparison of LER, LERcrop, and LER$_{PV}$ in Italy for different APV system designs as a function of row pitch.

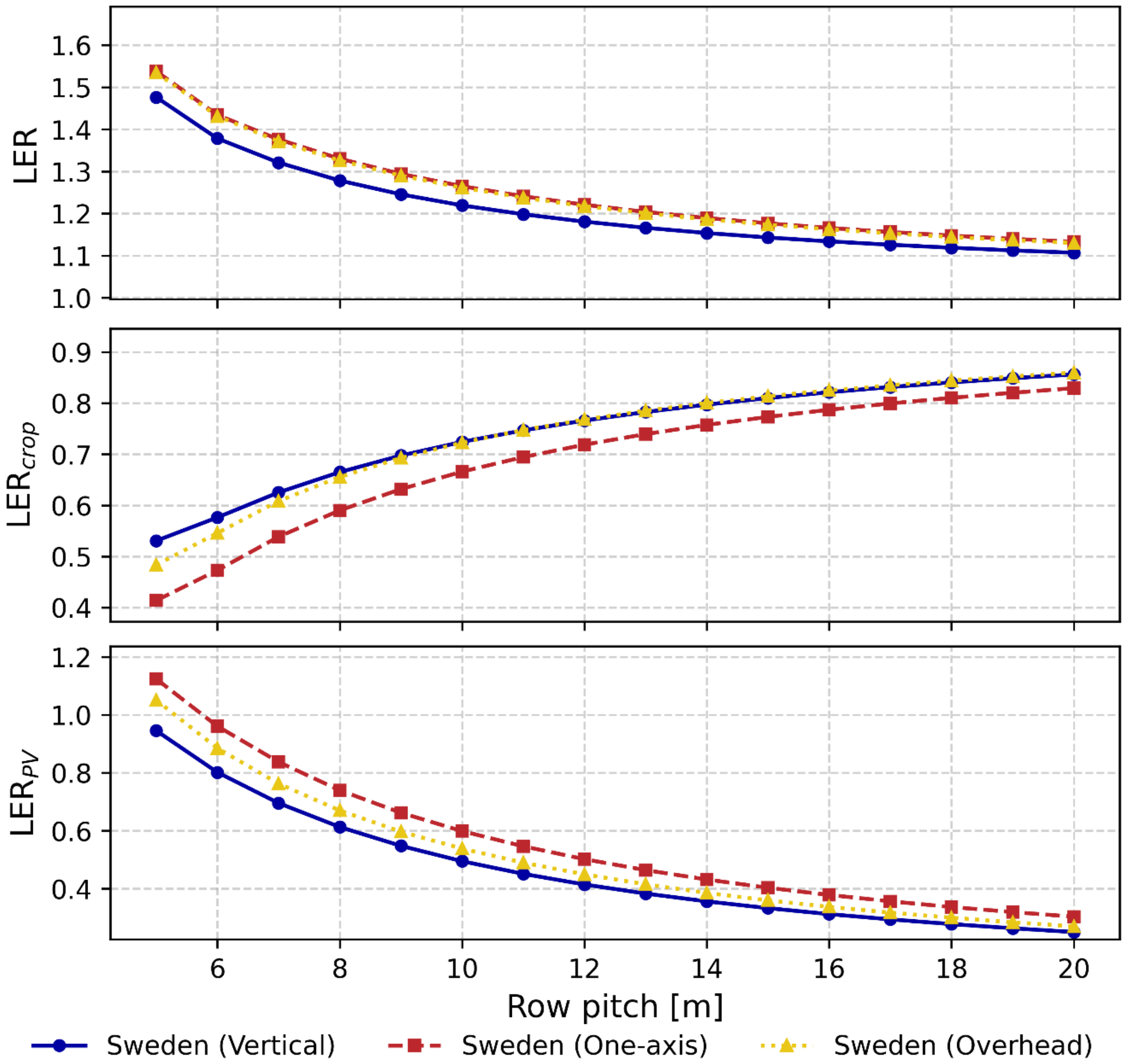

Figure A11. Comparison of LER, LERcrop, and LER_{PV} in Sweden for different APV system designs as a function of row pitch.

To validate the accuracy of the Agri-OptiCE® model, simulations were compared with outputs from the established bifacial_radiance [58] tool. Figure A12 presents a six-year comparison for Sweden (2018–2023) using a vertical bifacial layout with 0.5 m module height and 10 m row pitch. Seasonal averages of GHI and plane-of-array (POA) irradiance for both the front and rear side of module surfaces were evaluated. The results show strong agreement between the two models in both temporal trends and absolute irradiance values, supporting the reliability of Agri-OptiCE® for integrated APV analysis.

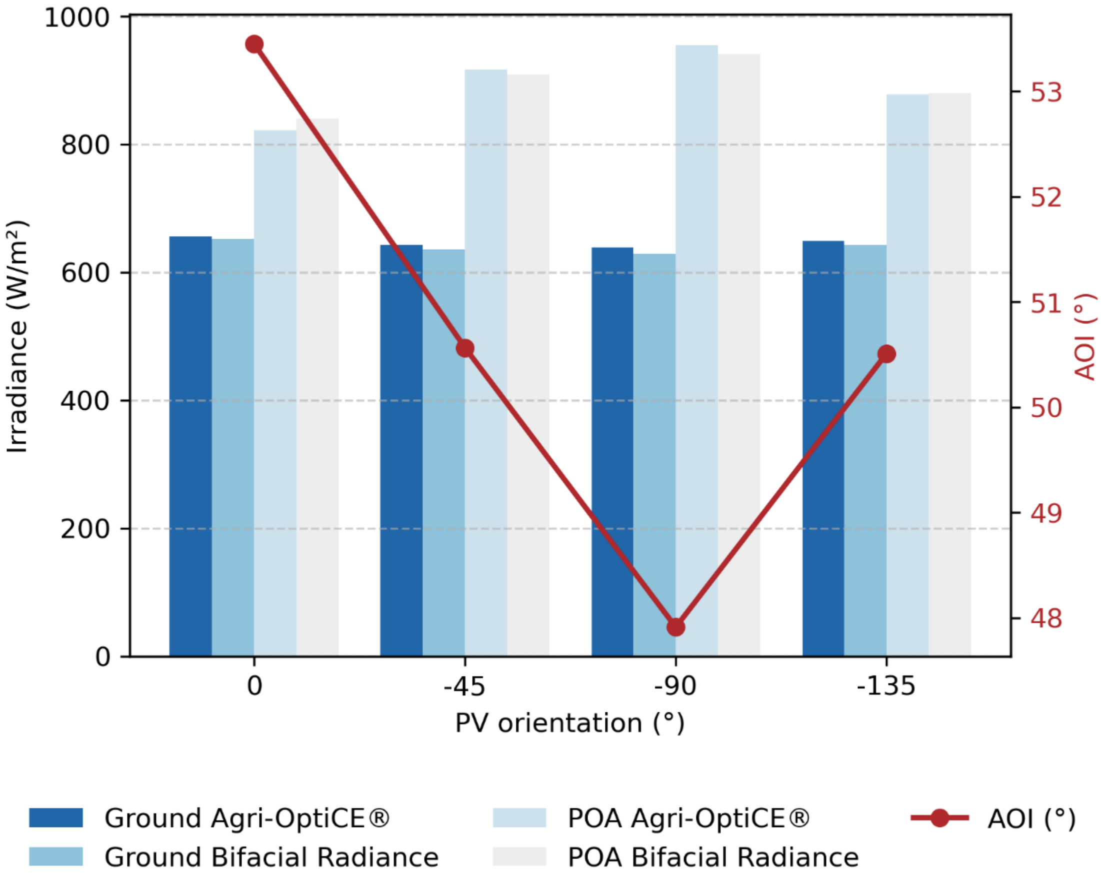

Figure A12. Validation of Agri-OptiCE® against bifacial_radiance for vertical systems in Sweden (2018–2023), showing PAR estimates averaged over harvesting periods.

References

[1] Gao D, Chen AS, Memon FA. A Systematic Review of Methods for Investigating Climate Change Impacts on Water-Energy-Food Nexus. Water Resour Manag 2024;38:1–43. https://doi.org/10.1007/s11269-023-03659-x.

[2] Water-Food-Energy Nexus | Land & Water | Food and Agriculture Organization of the United Nations | Land & Water | Food and Agriculture Organization of the United Nations 2024. https://www.fao.org/land-water/water/watergovernance/waterfoodenergynexus/en/ (accessed August 30, 2024).

[3] Campana PE, Zhang J, Yao T, Andersson S, Landelius T, Melton F, et al. Managing agricultural drought in Sweden using a novel spatially-explicit model from the perspective of water-food-energy nexus. J Clean Prod 2018;197:1382–93. https://doi.org/10.1016/j.jclepro.2018.06.096.

[4] Barron-Gafford GA, Pavao-Zuckerman MA, Minor RL, Sutter LF, Barnett-Moreno I, Blackett DT, et al. Agrivoltaics provide mutual benefits across the food–energy–water nexus in drylands. Nat Sustain 2019;2:848–55. https://doi.org/10.1038/s41893-019-0364-5.

[5] Jain P, Raina G, Sinha S, Malik P, Mathur S. Agrovoltaics: Step towards sustainable energy-food combination. Bioresour Technol Rep 2021;15:100766. https://doi.org/10.1016/j.biteb.2021.100766.

[6] Zhang Z, Zhang F, Zhang W, Li M, Liu W, Omer AAA, et al. Spectral-splitting concentrator agrivoltaics for higher hybrid solar energy conversion efficiency. Energy Convers Manag 2023;276:116567. https://doi.org/10.1016/j.enconman.2022.116567.

[7] Cheng C, Blakers A, Stocks M, Lu B. 100% renewable energy in Japan. Energy Convers Manag 2022;255:115299. https://doi.org/10.1016/j.enconman.2022.115299.

[8] Mamun MAA, Dargusch P, Wadley D, Zulkarnain NA, Aziz AA. A review of research on agrivoltaic systems. Renew Sustain Energy Rev 2022;161:112351. https://doi.org/10.1016/j.rser.2022.112351.
[9] Cuppari RI, Higgins CW, Characklis GW. Agrivoltaics and weather risk: A diversification strategy for landowners. Appl Energy 2021;291:116809. https://doi.org/10.1016/j.apenergy.2021.116809.
[10] Ayadi O, Al-Bakri JT, Abdalla MEB, Aburumman Q. The potential of agrivoltaic systems in Jordan. Appl Energy 2024;372:123841. https://doi.org/10.1016/j.apenergy.2024.123841.
[11] Elamri Y, Cheviron B, Lopez J-M, Dejean C, Belaud G. Water budget and crop modelling for agrivoltaic systems: Application to irrigated lettuces. Agric Water Manag 2018;208:440–53. https://doi.org/10.1016/j.agwat.2018.07.001.
[12] Dupraz C, Marrou H, Talbot G, Dufour L, Nogier A, Ferard Y. Combining solar photovoltaic panels and food crops for optimising land use: Towards new agrivoltaic schemes. Renew Energy 2011;36:2725–32. https://doi.org/10.1016/j.renene.2011.03.005.
[13] Jing R, Liu J, Zhang H, Zhong F, Liu Y, Lin J. Unlock the hidden potential of urban rooftop agrivoltaics energy-food-nexus. Energy 2022;256:124626. https://doi.org/10.1016/j.energy.2022.124626.
[14] Trommsdorff M, Kang J, Reise C, Schindele S, Bopp G, Ehmann A, et al. Combining food and energy production: Design of an agrivoltaic system applied in arable and vegetable farming in Germany. Renew Sustain Energy Rev 2021;140:110694. https://doi.org/10.1016/j.rser.2020.110694.
[15] Dinesh H, Pearce JM. The potential of agrivoltaic systems. Renew Sustain Energy Rev 2016;54:299–308. https://doi.org/10.1016/j.rser.2015.10.024.
[16] Sarr A, Soro YM, Tossa AK, Diop L. A new approach for modelling photovoltaic panel configuration maximizing crop yield and photovoltaic array outputs in agrivoltaics systems. Energy Convers Manag 2024;309:118436. https://doi.org/10.1016/j.enconman.2024.118436.
[17] Willockx B, Reher T, Lavaert C, Herteleer B, Van De Poel B, Cappelle J. Design and evaluation of an agrivoltaic system for a pear orchard. Appl Energy 2024;353:122166. https://doi.org/10.1016/j.apenergy.2023.122166.
[18] Kwon O, Kang J, Trommsdorff M, Lee K. Sensitivity Analysis for Optimized Agrivoltaic Designs: An Inquiry on the Trade-off Between Homogenous Light Conditions and Electrical Yield. 2020 47th IEEE Photovolt. Spec. Conf. PVSC, Calgary, AB, Canada: IEEE; 2020, p. 1220–5. https://doi.org/10.1109/PVSC45281.2020.9300677.
[19] Trommsdorff M, Kang J, Reise C, Schindele S, Bopp G, Ehmann A, et al. Combining food and energy production: Design of an agrivoltaic system applied in arable and vegetable farming in Germany. Renew Sustain Energy Rev 2021;140:110694. https://doi.org/10.1016/j.rser.2020.110694.
[20] Campana PE, Stridh B, Amaducci S, Colauzzi M. Optimisation of vertically mounted agrivoltaic systems. J Clean Prod 2021;325:129091. https://doi.org/10.1016/j.jclepro.2021.129091.
[21] Miljkovic N, Du X, Solecki A, Hoque MJ, Garimella VS, Jia M, et al. Advancing Agrivoltaics through a Systematic Design Framework: Guidelines for Integration and Informed Decision-Making 2024. https://doi.org/10.21203/rs.3.rs-4791170/v1.
[22] Setchell H. ECMWF Reanalysis v5 2020.
[23] Myers DR, Stoffel TL, Reda I, Wilcox SM, Andreas AM. Recent Progress in Reducing the Uncertainty in and Improving Pyranometer Calibrations. J Sol Energy Eng 2002;124:44–50. https://doi.org/10.1115/1.1434262.
[24] Erbs DG, Klein SA, Duffie JA. Estimation of the diffuse radiation fraction for hourly, daily and monthly-average global radiation. Sol Energy 1982;28:293–302. https://doi.org/10.1016/0038-092X(82)90302-4.
[25] Ferrera-Cobos F, Vindel JM, Valenzuela RX, González JA. Analysis of Spatial and Temporal Variability of the PAR/GHI Ratio and PAR Modeling Based on Two Satellite Estimates. Remote Sens 2020;12:1262. https://doi.org/10.3390/rs12081262.
[26] Ma Lu S, Zainali S, Stridh B, Avelin A, Amaducci S, Colauzzi M, et al. Photosynthetically active radiation decomposition models for agrivoltaic systems applications. Sol Energy 2022;244:536–49. https://doi.org/10.1016/j.solener.2022.05.046.

[27] Zainali S, Ma Lu S, Stridh B, Avelin A, Amaducci S, Colauzzi M, et al. Direct and diffuse shading factors modelling for the most representative agrivoltaic system layouts. Appl Energy 2023;339:120981. https://doi.org/10.1016/j.apenergy.2023.120981.
[28] Campana PE, Stridh B, Hörndahl T, Svensson S-E, Zainali S, Lu SM, et al. Experimental results, integrated model validation, and economic aspects of agrivoltaic systems at northern latitudes. J Clean Prod 2023:140235. https://doi.org/10.1016/j.jclepro.2023.140235.
[29] Campana P, Staaf Scragg J, Ma Lu S, Zainali S, Stridh B, Amaducci S, et al. Solar irradiance distribution under vertically mounted agrivoltaic systems – Model development, validation, and applications for microclimate assessment. Agriculture; 2022. https://doi.org/10.31223/X5G07D.
[30] Ma Lu S, Zainali S, Sundström E, Nygren A, Stridh B, Avelin A, et al. Validation of Vertical Bifacial Agrivoltaic and Other Systems Modelling: Effect of Dynamic Albedo on Irradiance and Power Output Estimations. AgriVoltaics Conf Proc 2024;2. https://doi.org/10.52825/agripv.v2i.1004.
[31] Huasun HJT Solar Module For Sale, Bifacial Solar Panel Manufacturer. Anhui Huasun Energy Co Ltd 2025. https://www.huasunsolar.com/products/hjt-solar-module/ (accessed March 25, 2025).
[32] Beed FD, Paveley ND, Sylvester-Bradley R. Predictability of wheat growth and yield in light-limited conditions. J Agric Sci 2007;145:63–79. https://doi.org/10.1017/S0021859606006678.
[33] Reher T, Lavaert C, Willockx B, Huyghe Y, Bisschop J, Martens JA, et al. Potential of sugar beet (Beta vulgaris) and wheat (Triticum aestivum) production in vertical bifacial, tracked, or elevated agrivoltaic systems in Belgium. Appl Energy 2024;359:122679. https://doi.org/10.1016/j.apenergy.2024.122679.
[34] Laub M, Pataczek L, Feuerbacher A, Zikeli S, Högy P. Contrasting yield responses at varying levels of shade suggest different suitability of crops for dual land-use systems: a meta-analysis. Agron Sustain Dev 2022;42:51. https://doi.org/10.1007/s13593-022-00783-7.
[35] Edouard S, Combes D, Van Iseghem M, Ng Wing Tin M, Escobar-Gutiérrez AJ. Increasing land productivity with agriphotovoltaics: Application to an alfalfa field. Appl Energy 2023;329:120207. https://doi.org/10.1016/j.apenergy.2022.120207.
[36] J. R. Williams, C. A. Jones, J. R. Kiniry, D. A. Spanel. The EPIC Crop Growth Model. Trans ASAE 1989;32:0497–511. https://doi.org/10.13031/2013.31032.
[37] EPIC & APEX Models 2025. https://epicapex.tamu.edu/ (accessed March 25, 2025).
[38] Bellone Y, Croci M, Impollonia G, Nik Zad A, Colauzzi M, Campana PE, et al. Simulation-Based Decision Support for Agrivoltaic Systems. Appl Energy 2024;369:123490. https://doi.org/10.1016/j.apenergy.2024.123490.
[39] Instruktion för bedömning av stödberättigad jordbruksmark 2024.
[40] DIN SPEC 91434:2021-05, Agri-Photovoltaik-Anlagen_- Anforderungen an die landwirtschaftliche Hauptnutzung 2025. https://doi.org/10.31030/3257526.
[41] Vollprecht J, Trommsdorff M. New Legal Framework of Agrivoltaics in Germany. AgriVoltaics Conf Proc 2024;2. https://doi.org/10.52825/agripv.v2i.1071.
[42] Max Trommsdorff, Jens Vollprecht. Current legal framework for agrivoltaics in Germany 2023.
[43] Italy publishes new national guidelines for agrovoltaic plants. Pv Mag Int 2022. https://www.pv-magazine.com/2022/07/05/italy-publishes-new-national-guidelines-for-agrovoltaic-plants/ (accessed March 25, 2025).
[44] Ministero dell'Ambiente e della Sicurezza Energetica. Linee Guida in materia di Impianti Agrivoltaici. Ministero dell'Ambiente e della Sicurezza Energetica; 2022.
[45] Ministero dell'Ambiente e della Sicurezza Energetica. Agrivoltaico - Criteri e modalità per incentivare la realizzazione di sistemi agrivoltaici di natura sperimentale 2023.
[46] Laura Svanera, Stefano Amaducci, Michele Colauzzi, Girolamo Di Francia, Giancarlo Ghidesi, Salvatore Guastella, et al. Sistemi agrivoltaici - Integrazione di attività agricole e impianti fotovoltaici. UNI - Ente Italiano di Normazione; 2023.
[47] El-Gafy I. Water–food–energy nexus index: analysis of water–energy–food nexus of crop's production system applying the indicators approach. Appl Water Sci 2017;7:2857–68. https://doi.org/10.1007/s13201-017-0551-3.

[48] Hassanat A, Almohammadi K, Alkafaween E, Abunawas E, Hammouri A, Prasath VBS. Choosing Mutation and Crossover Ratios for Genetic Algorithms—A Review with a New Dynamic Approach. Information 2019;10:390. https://doi.org/10.3390/info10120390.
[49] Gao S, Wang K, Tao S, Jin T, Dai H, Cheng J. A state-of-the-art differential evolution algorithm for parameter estimation of solar photovoltaic models. Energy Convers Manag 2021;230:113784. https://doi.org/10.1016/j.enconman.2020.113784.
[50] Zidane TEK, Zainali S, Bellone Y, Guezgouz M, Khosravi A, Ma Lu S, et al. Economic evaluation of one-axis, vertical, and elevated agrivoltaic systems across Europe: a Monte Carlo Analysis. Appl Energy 2025;391:125826. https://doi.org/10.1016/j.apenergy.2025.125826.
[51] Yang JM, Yang JY, Liu S, Hoogenboom G. An evaluation of the statistical methods for testing the performance of crop models with observed data. Agric Syst 2014;127:81–9. https://doi.org/10.1016/j.agsy.2014.01.008.
[52] Jones JW, Hoogenboom G, Porter CH, Boote KJ, Batchelor WD, Hunt LA, et al. The DSSAT cropping system model. Eur J Agron 2003;18:235–65. https://doi.org/10.1016/S1161-0301(02)00107-7.
[53] Gou F, Van Ittersum MK, Simon E, Leffelaar PA, Van Der Putten PEL, Zhang L, et al. Intercropping wheat and maize increases total radiation interception and wheat RUE but lowers maize RUE. Eur J Agron 2017;84:125–39. https://doi.org/10.1016/j.eja.2016.10.014.
[54] Dos Santos Neto A, Panozzo A, Piotto S, Mezzalira G, Furlan L, Vamerali T. Screening old and modern wheat varieties for shading tolerance within a specialized poplar plantation for agroforestry farming systems implementation. Agrofor Syst 2024;98:2765–83. https://doi.org/10.1007/s10457-024-00956-1.
[55] Arenas-Corraliza MG, Rolo V, López-Díaz ML, Moreno G. Wheat and barley can increase grain yield in shade through acclimation of physiological and morphological traits in Mediterranean conditions. Sci Rep 2019;9:9547. https://doi.org/10.1038/s41598-019-46027-9.
[56] Cruz P. Effect of shade on the growth and mineral nutrition of a C4 perennial grass under field conditions. Plant Soil 1997;188:227–37. https://doi.org/10.1023/A:1004296622463.
[57] Stein JS, Maugeri G, Ovaitt S, Müller T. Bifacial PV Systems with Tracking: Analysis and Field Experience. International Energy Agency Photovoltaic Power Systems Programme (IEA-PVPS); 2024.
[58] Ayala Pelaez S, Deline C. bifacial_radiance: a python package for modeling bifacial solar photovoltaic systems. J Open Source Softw 2020;5:1865. https://doi.org/10.21105/joss.01865.
[59] Marrou H, Wery J, Dufour L, Dupraz C. Productivity and radiation use efficiency of lettuces grown in the partial shade of photovoltaic panels. Eur J Agron 2013;44:54–66. https://doi.org/10.1016/j.eja.2012.08.003.
[60] Sieber P, Böhme S, Ericsson N, Hansson P-A. Albedo on cropland: Field-scale effects of current agricultural practices in Northern Europe. Agric For Meteorol 2022;321:108978. https://doi.org/10.1016/j.agrformet.2022.108978.
[61] Ferry A, Parenti M, Thebault M, Ménézo C, Fossa M. Optimal tilt angles for bifacial photovoltaic plants across Europe based on cumulative sky and Typical Meteorological Year data. Sol Energy 2025;293:113475. https://doi.org/10.1016/j.solener.2025.113475.
[62] Saint-Drenan Y-M, Wald L, Ranchin T, Dubus L, Troccoli A. An approach for the estimation of the aggregated photovoltaic power generated in several European countries from meteorological data. Adv Sci Res 2018;15:51–62. https://doi.org/10.5194/asr-15-51-2018.
[63] Escribano M, Gaspar P, Mesias FJ. Creating market opportunities in rural areas through the development of a brand that conveys sustainable and environmental values. J Rural Stud 2020;75:206–15. https://doi.org/10.1016/j.jrurstud.2020.02.002.
[64] Aspeteg J, Bergek A. The value creation of diffusion intermediaries: Brokering mechanisms and trade-offs in solar and wind power in Sweden. J Clean Prod 2020;251:119640. https://doi.org/10.1016/j.jclepro.2019.119640.
[65] Sturchio MA, Kannenberg SA, Knapp AK. Agrivoltaic arrays can maintain semi-arid grassland productivity and extend the seasonality of forage quality. Appl Energy 2024;356:122418. https://doi.org/10.1016/j.apenergy.2023.122418.

[66] Baleta J, Mikulčić H, Klemeš JJ, Urbaniec K, Duić N. Integration of energy, water and environmental systems for a sustainable development. J Clean Prod 2019;215:1424–36. https://doi.org/10.1016/j.jclepro.2019.01.035.
[67] Trommsdorff M, Hopf M, Hörnle O, Berwind M, Schindele S, Wydra K. Can synergies in agriculture through an integration of solar energy reduce the cost of agrivoltaics? An economic analysis in apple farming. Appl Energy 2023;350:121619. https://doi.org/10.1016/j.apenergy.2023.121619.
[68] Trommsdorff M, Campana PE, Macknick J, Fernández Solas A, Gorjian S, Tsanakas I. Dual Land Use for Agriculture and Solar Power Production: Overview and Performance of Agrivoltaic Systems. International Energy Agency Photovoltaic Power Systems Programme; 2025. https://doi.org/10.69766/XAEU5008.